DETERMINING THE DEPOSITIONAL ENVIRONMENT OF THE LOWER EAGLE FORD IN LOZIER CANYON, ANTONIO CREEK, AND OSMAN CANYON, TEXAS: AN OUTCROP STUDY OF BEDDING FEATURES AT OUTCROP SCALE

A Thesis

by

TREY SAXON LYON

Submitted to the Office of Graduate and Professional Studies of
Texas A&M University
in partial fulfillment of the requirements for the degree of

MASTER OF SCIENCE

Chair of Committee,	John R. Giardino
Committee Members,	Michael C. Pope
	Juan Carlos Laya
	Chris Houser
Head of Department,	John R. Giardino

May 2015

Major Subject: Geology

ABSTRACT

The Eagle Ford Formation is currently the most economically significant unconventional resource play in the state of Texas. There has been much debate as to the environment of deposition for the lowermost Facies A of the Eagle Ford in outcrop exposures in Lozier Canyon, Texas. Two conflicting hypotheses were proposed: 1) Sedimentary structures in Facies A are hummocky cross-stratification (HCS) and swaley cross-stratification (SCS), which indicates a shelfal depositional environment above the storm wave base (SWB). 2) Sedimentary structures in Facies A are a mixture of diagenetically separated contourites, turbidites, and pinch-and-swell beds, which indicate a distal-slope depositional environment below SWB. This research used field work, three-dimensional analysis of sedimentary structures, measurements of ripple height, and laboratory analysis to interpret the environment of deposition. The results of these observations and data suggest that the sedimentary structures in Facies A record a depositional environment above SWB.

Observation of cross-bedded structures in three-dimensions reveals (i) isotropic truncation of laminae; (ii) symmetric rounded ripples; (iii) large variations in laminae geometry, truncation, and dip inclination, attributed to fluctuations in storm intensity, frequency, and duration; and (iv) and bidirectional downlap and reactivation surfaces associated with oscillatory flow above the SWB.

This study interprets cross-bedded sedimentary structures in Facies A as swaley cross-stratification (SCS) and hummocky cross-stratification (HCS) associated with

storm events, and thus places Facies A in a depositional environment above storm wave-base (SWB).

ACKNOWLEDGEMENTS

I would like to thank my committee chair, Dr. Giardino, and my committee members, Dr. Pope, Dr. Laya, and Dr. Houser, for their guidance and support throughout the course of this research.

Thanks to my friends, colleagues, and the department faculty and staff for making my time at Texas A&M University a great experience. I also want to extend my gratitude to the BP America Corporation, which provided the funds, land access, and equipment for this study. Thanks to the Fort Worth D&D Club for awarded scholarships that allowed me to continue my research.

Field assistance was generously provided by Matthew Wehner, Bronwyn Moore and Andrew Philbin. Special thanks to Matthew Wehner, Paul Myrow, Mauricio Perillo, Ryan Ewing, Michael Tice, and Roger Higgs for collaboration and invaluable insight to questions pertaining to this study.

Finally, thanks to my mother and father for their support and wisdom, and to my wife for her unending encouragement and optimism.

TABLE OF CONTENTS

Page

LIST OF FIGURES

1. INTRODUCTION

The Late Cretaceous Eagle Ford Formation currently is the most active unconventional shale play in the world, with over $30 billion invested in 2013 and 260 rigs currently in operation (U.S. Energy Information Administration, 2014). Outcrop exposures of the Eagle Ford extend from north Texas through Waco, Austin, San Antonio and into Mexico. The best exposures of Maverick Basin deposits occur in Antonio Creek and Lozier Canyon in Del Rio, Texas (Figure 1). The depositional environment of lowermost outcrop facies in the Eagle Ford still remains controversial as to whether Facies A was deposited above or below storm wave-base (SWB). Outcrop samples were taken from Lozier Canyon, Antonio Creek, and Osman Canyon for this study. LiDAR scans were also taken throughout Lozier Canyon and Antonio Creek to determine the usefulness of LiDAR for quantitative data collection at the outcrop scale. Outcrop exposures in west Texas and subsurface studies of the Eagle Ford (Boquillas) Group have allowed geologists to determine facies, biostratigraphy, cycles, and lateral facies distribution (Adkins and Lozo 1951, Freeman 1961, 1968, Dawson 2000, Lock and Piescher 2006, Donovan and Staerker 2010, Donovan et al. 2012, Gardner et al. 2013, Wehner 2013*)*. Lozier Canyon is an ideal location to compare and contrast bedding features in Facies A because it exposes a complete vertical section of the Eagle Ford over a large lateral extent. The lowest beds of the Eagle ford Group and the contact of Facies A in the Eagle Ford Group with the underlying Buda Formation is exposed for miles, which provides the ability to compare and contrast its 2-D and 3-D bedding

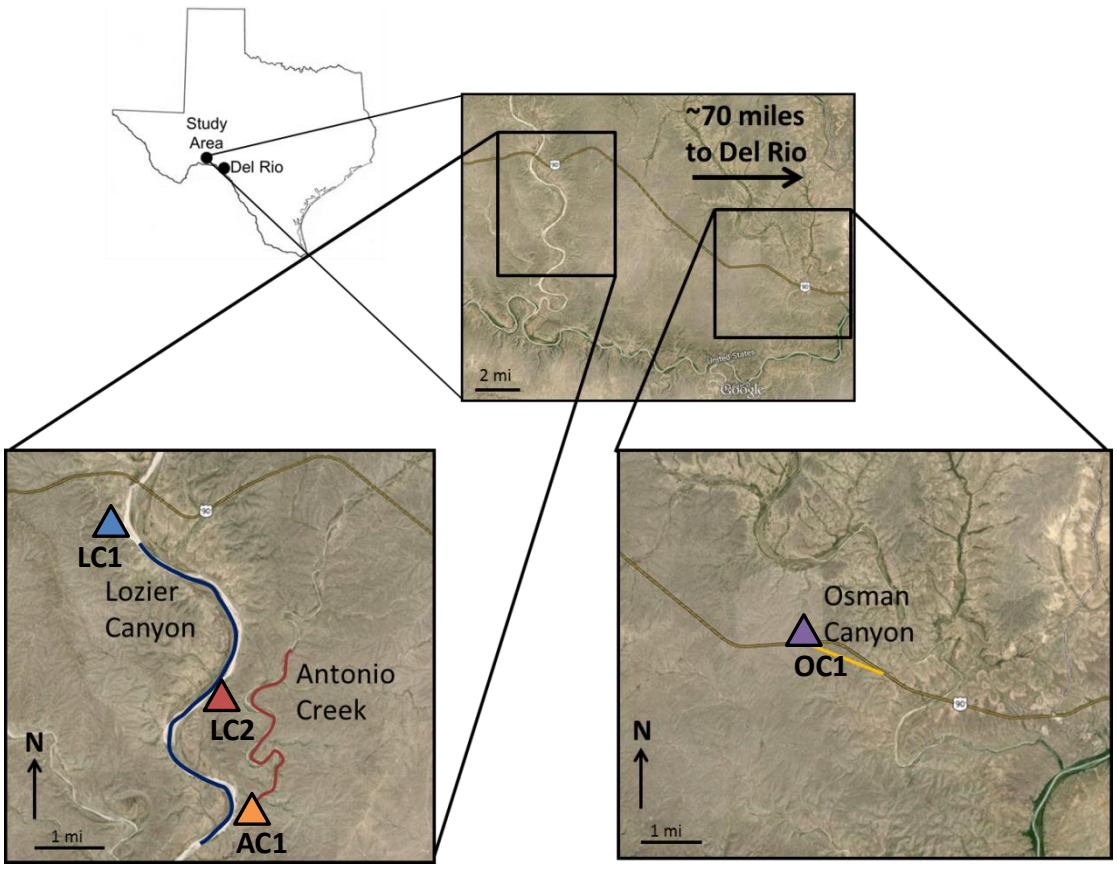

Figure 1. Location of study areas in Lozier Canyon, Antonio Creek, and Osman Canyon. Triangles represent locations where samples and detailed outcrop pictures were taken.

features over a large lateral extent. Studies of these outcrops indicate that the Eagle Ford Group in west Texas consists of a transgressive lower member and a regressive upper member (Donovan and Staerker 2010). The Eagle Ford Group was sub-divided into five facies (A-E) based on lithology, biostratigraphy, and characteristic log signatures (Donovan et al. 2012, Gardner et al. 2013).

The basal transgressive unit, Facies A, was deposited on an unconformity above the underlying Buda Formation and is not present in the subsurface to the south. Although the Eagle Ford Group was extensively studied at outcrops in west Texas (Freeman 1961, Trevino 1988, 2002, Dawson 2000, Lock and Peschier 2006, 2010, Ruppel et al. 2012, Donovan and Staerker 2010, 2012, Gardner et al. 2013, Wehner et al 2013), the depositional environment for the lower Eagle Ford remains controversial.

Facies A, composed of fine-grained foraminiferal grainstone and packstone, commonly has small three-dimensional sedimentary structures in the outcrop belt, but these features do not occur in the subsurface to the southeast (Figure 2). Most beds in Facies A pinch out or are scoured over several meters and are laterally discontinuous. However, bedding thickness and the styles of cross-bedding are similar throughout the region based on outcrop observation throughout Lozier Canyon and at numerous road-cuts along Texas Highway 90. These amalgamated skeletal grainstone and packstone beds range from 2 cm to 25 cm thick and are separated by thin organic-rich mudstone layers (0.5 cm to 8 cm thick), with sparse bentonite beds (< 3 cm thick). Facies A is approximately 6 m (20 ft) thick in Antonio Creek, Lozier Canyon, and in exposures along Texas Highway 90 near Langtry, TX (Figure 1).

Two types of sedimentary structures in Facies A were studied to determine its depositional environment: cross-bedded samples and contorted beds. The primary focus of this study was to measure and analyze small (< 15 cm) cross-bedded sedimentary structures that are ubiquitous in Facies A. These beds were sampled, measured, and cut into blocks in order to understand the processes responsible for their deposition.

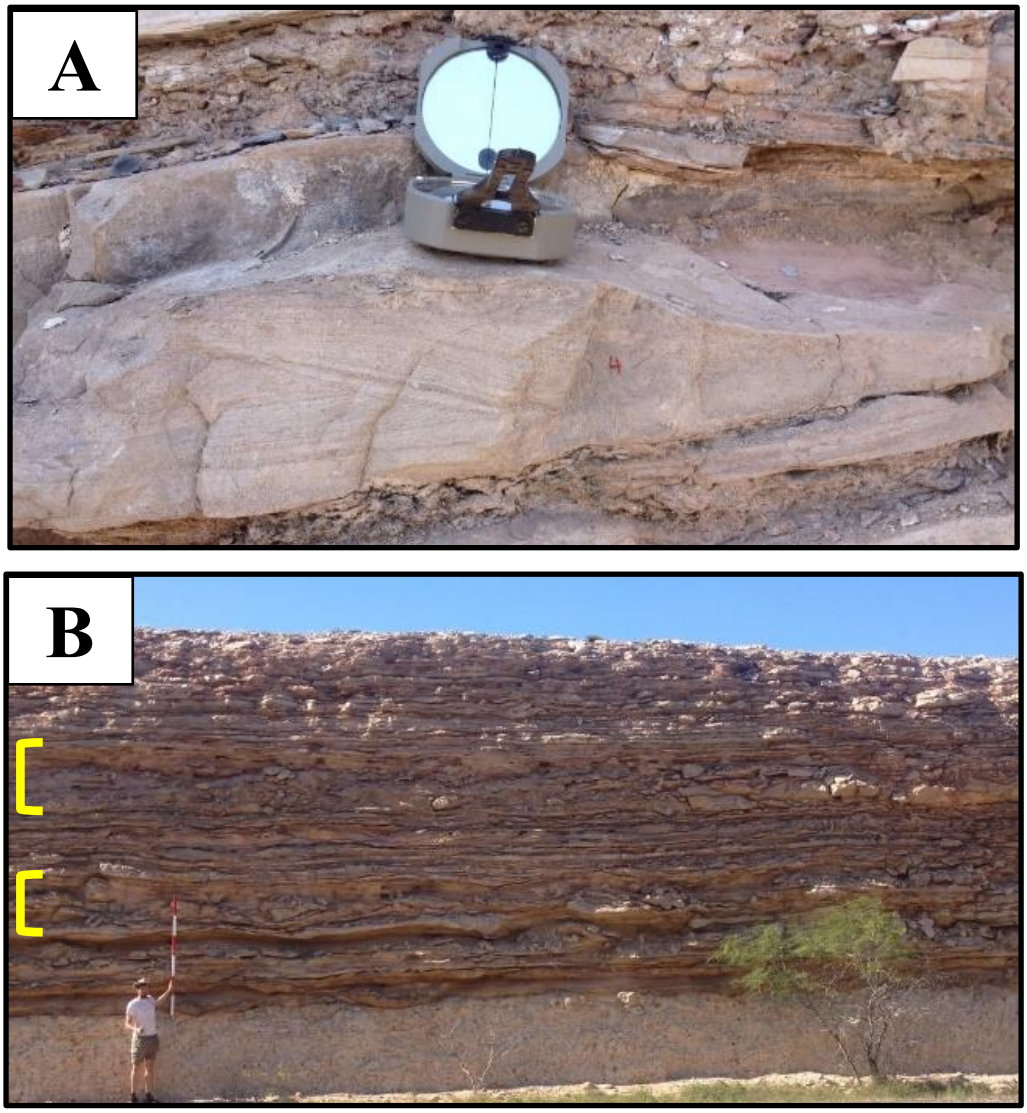

Figure 2. Sedimentary structures in Facies A. (A) Uninterpreted three-dimensional view of sedimentary structures. These structures are the focus of this study. This Facies A sample is located in Antonio Creek (AC1). Contorted beds (brackets) located along Texas Highway 90. These beds indicate movement of large amounts of sediment over a short distance. Two distinct contorted beds can be observed in Facies A at multiple locations along Texas Highway 90 and in Lozier Canyon. The conflicting interpretations for these deposits suggest that the character of this bedding is the result of seismic liquefaction or mass transport debris flows.

Large contorted beds (Figure 2b) within Facies A outcrop in Antonio Creek, Lozier Canyon, and along Highway 90, but are not the primary focus of this study because they are less diagnostic of depositional environment. Description and detailed photography at the outcrop scale was used to determine the mechanisms that created these deformation features. Observation of deformation provides insights into mechanisms that caused the deformation and the depositional environment in which they formed. The contorted beds are widespread and laterally discontinuous throughout the outcrop belt of Del Rio based on observations in Lozier Canyon, Antonio Creek, Osman Canyon, and other road outcrops along Texas Highway 90.

Difficulties in interpreting the cross-bedding in Facies A of the Eagle Ford Group have led to two disparate interpretations; either as HCS and SCS deposited in a shallow-water environment above SWB (Trevino 1988, 2002, Donovan and Staerker 2010, Donovan et al. 2012, Gardner et al. 2013, Bohacs 2014), or as pinch-and-swell beds, traction deposits, distorted turbidites, and contourite ripples that were modified by diagenetic segregation and compaction on a distal-ramp setting (Freeman 1961, 1968, Lock and Peschier 2006, Lock et al. 2010, Ruppel et al. 2012). A similar interpretation by Ruppel et al. (2012) stated that cross-bedded structures in Facies A are deep-water "HCS-like" antidune structures similar to those described by Mulder et al. (2009). These structures were interpreted to be Tb-Td Bouma turbidite intervals that were modified by standing waves at the upper-flow face of a turbidity current in a deep-water slope setting on the drowned Lower Cretaceous shelf (Ruppel et al 2012).

The current study presents detailed observations and measurements of a suite of sedimentary structures in Facies A samples from Lozier Canyon and Antonio Creek. These samples were cut and measured, showing laminae dips that are highly variable in dip angle (10°-35°), wavelength, and bedding character. Collected data and observations suggest that the cross-bedding in Facies A is primarily small-scale SCS and HCS, and oscillatory wave-ripples associated with storm deposition, all of which are indicative of a shelfal depositional environment above SWB (Greenwood and Sherman 1986).

2. GEOLOGIC SETTING

During the Early Cretaceous the Comanche Platform (Figure 3) developed across most of Central Texas in the Western Interior Seaway (WIS). The platform-margin reef buildups on the Comanche Platform are known as the Stuart City and Santa Elena Reef trends. These reefs greatly controlled the extent of deposition and physiography of the overlying Eagle Ford Group (Donovan and Staerker, 2010).

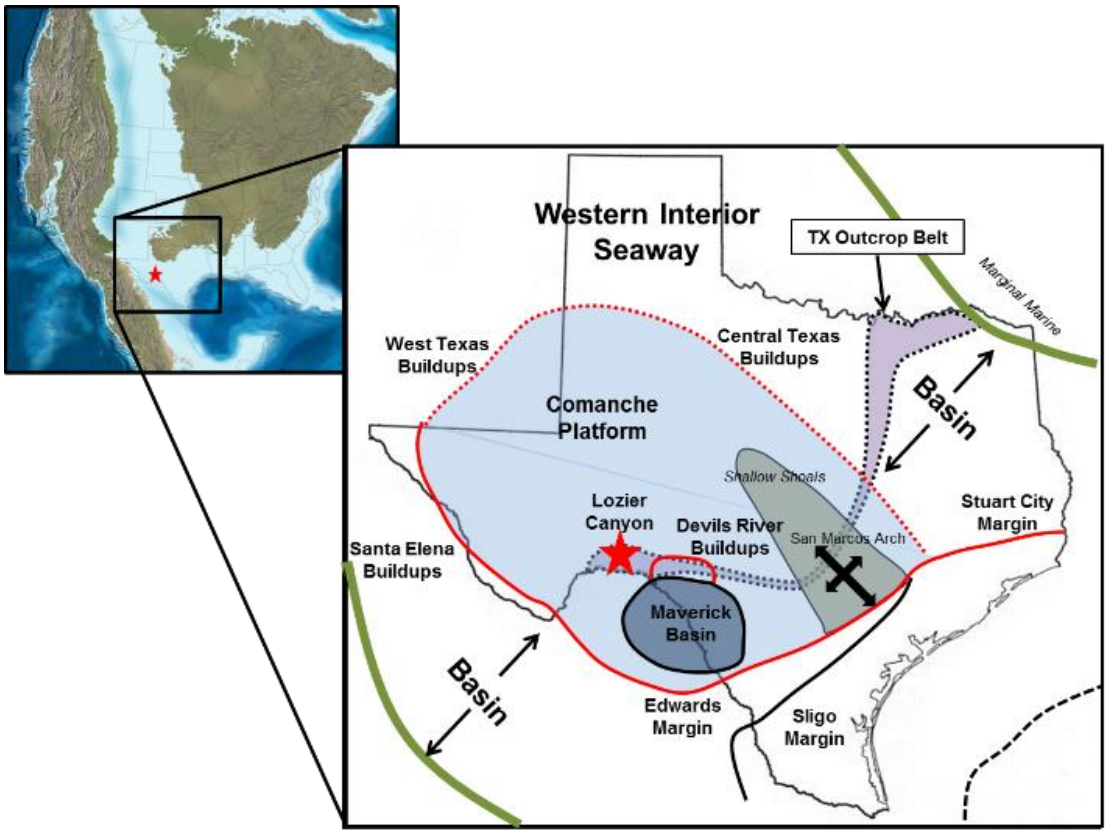

Figure 3. Generalized paleogeographic map. This figure depicts Eagle Ford depocenters in the late Cenomanian. Regional geology map modified from Donovan and Staerker (2010). Western Interior Seaway map modified from Blakey (1989).

Deposition of Eagle Ford outcrops in west Texas coincided with periods of flooding and deposition of thick organic-rich sediment packages on the Comanche Platform and in the troughs of reef buildups in the Late Cretaceous. (Lehman et al. 2000, Donovan et al. 2012). Facies A is the lowermost facies of the Eagle Ford and was deposited in a transgressive systems tract (TST) over the Buda Formation.

Several hypotheses which have been proposed are in disagreement about the geologic setting at the time of deposition of Facies A. One group of researchers led by Donovan and Staerker (2010) propose that cross-bedded structures in Facies A are HCS and SCS and thus were deposited on a relatively flat carbonate shelf above SWB (Trevino 1988, Donovan and Staerker 2010, 2012, Gardner et al. 2013). Conversely, it was proposed by Lock and Peschier (2006, 2010) and Ruppel et al. (2012) that cross-bedded structures in Facies A are formed by deep-water density currents and thus were deposited on a deeper water slope setting below SWB (Lock and Peschier 2006, 2010, Ruppel et al. 2012)

3. BACKGROUND

The current study utilizes observations and data gathered from the field and in the laboratory to compare and contrast cross-bedded sedimentary structures in Facies A with analogous depositional models and sedimentary structures (Myrow and Southard 1991, Myrow et al. 2002, Dumas and Arnott 2006) . The data generated in this study were compared with combined storm-flow deposits of HCS and SCS (Harms et al. 1975; Bourgeois; 1980, Dott and Bourgeois; 1982, Leckie and Walker 1982; Aigner 1985; Midtgaard 1996, Molgat and Arnott 2001) and ancient and modern deep-water contourites, turbidites, and antidunes (Bouma 1962, 1972; Middleton 1965; Heezen et al.1966; Hollister and Heezen 1972; Barwis and Hayes 1985; Rust and Gibling 1990; Duan et al. 1993; Alexander et al. 2001; Brackenridge et al. 2011; Cartigny et al. 2014).

3.1 Tempestites and HCS/SCS

Criteria for interpreting cross-bedding as HCS (Figure 4) are; i) large-scale wavelengths of 1-5 m and heights up to 0.5 m; (ii) isotropic stratification with no clear orientation; (iii) structures containing lower bounding erosional surfaces that dip at low angles of approximately 10°; (iv) laminations that thicken into crests and thin laterally into troughs; (v) dip of internal laminations normally decrease upwards (Harms et al. 1975).

Criteria for HCS in carbonate tempestites is slightly different than criteria used for sand-dominated tempestite deposits. HCS in carbonate tempestites consists of; (i) basal shell-lag and rip-up clasts; (ii) low angle stratification and irregular bedding; (iii) small hummocks with wavelengths on the dm- to- cm scale and amplitudes of 1-3 cm; (iv) occasional graded packstone rhythmites at the upper and/or lower bounds of HCS truncations (Kreisa 1981, Aigner 1985, Sageman 1996, Molina et al. 1997).

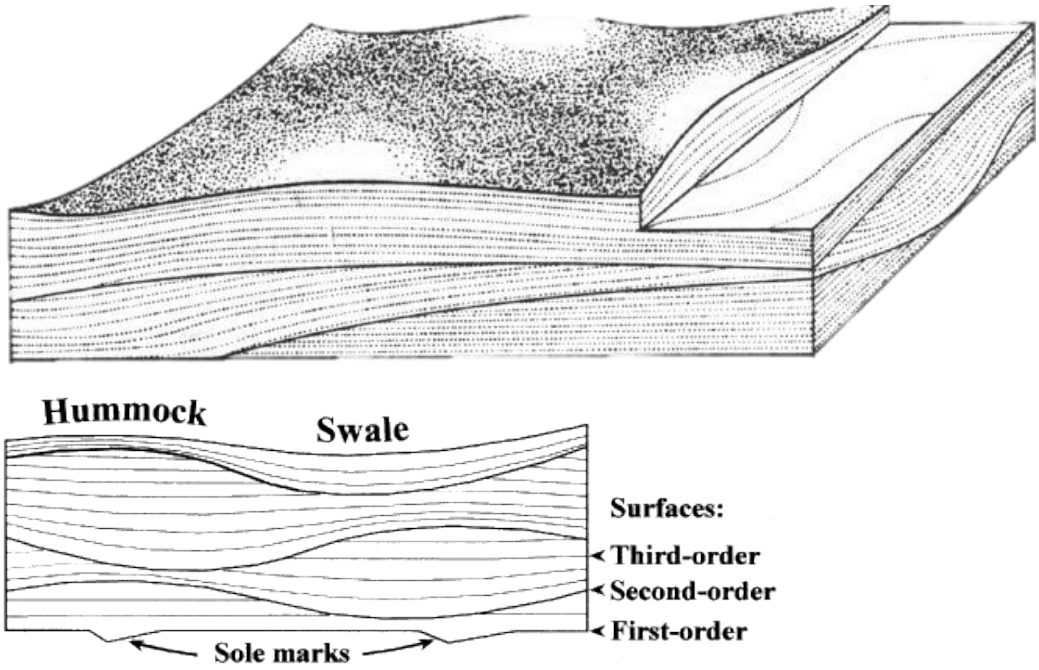

Figure 4. Idealized hummocky cross-stratification in 3-D. Modified from Harms et al. (1975). Idealized HCS consists of isotropically dipping laminae, mounds at the upper surface, and concave-up swaley cross-stratification in troughs.

3.2 Small-Scale HCS

Sedimentary structures resembling small-scale HCS similar to bedforms in the Eagle Ford Group Facies A can form as deep-water turbidites with antidune stratification (Prave and Duke 1991, Mulder et al. 2009, 2011). Small-scale HCS-like structures in the Hayzabia Flysch sequence (Western Pyrenees, France) were interpreted as Tc interval turbidites that were reworked by standing waves from the Kelvin-Helmholtz instability at the upper-flow interface (Mulder et al. 2009, 2011). The Kelvin-Helmholtz (K-H) instability occurs at the horizontal interface in parallel shear flows moving at different speeds or directions. Once the shear strength of the laminar interface is overcome by the frictional force between the two fluids, penetration of one fluid layer into the other takes place in the form of a wave, vortex, or billow. For a turbidity current, it is proposed that once erosion ceases and deposition begins, a standing or up-dip migrating surface wave is caused by the K-H instability (Mulder et al. 2009, 2011). It is proposed that the up-dip migration caused by the K-H instability forms antidune structures that are similar to HCS (Mulder et al. 2009, 2011). There are no other published reports of HCS or HCS-like features linked to deep-water deposition and the description of the origin of the proposed upper flow-face instabilities remains unproven (Higgs 2011, Quin 2011).

In contrast, small-scale HCS commonly is associated as tempestite storm deposits, suggesting that small-scale HCS is merely a result of the wide variety of depositional and erosional processes associated with storm events on a shelfal environment above SWB (e.g. DeRaaf et al 1977, Kreisa 1981b, Aigner 1982, 1985,

Allen 1982, Walker et al. 1983, Swift et al. 1983, Nottvedt and Kreisa 1987, Craft and Bridge 1987, Duke 1990, Duke et al. 1991, Myrow and Southard 1996, Seguret et al 2001, Mrinjek 2005, Higgs 2011). Distinguishing between tempestites and turbidites can be difficult because HCS and SCS in storm deposits often resemble Tb-Td intervals in turbidite successions because of the nature of their sudden high-energy deposition and graded character (Hamblin and Walker 1979, Leckie and Walker 1982).

Difficulties also exist in differentiating between HCS and antidunes, because both structures have low-angle stratification and three-dimensional bedforms, often resembling one another at the outcrop scale (Prave and Duke 1990, Rust and Gibling 1990, Alexander et al. 2001, Quin 2011, Cartigny et al. 2014). However, distinctions between HCS, turbidites, and antidunes can still be made based on the evidence or lack thereof of oscillatory flow in turbidites/antidunes (Hunter and Clifton 1981, Christie-Blick et al. 1990, Einsele et al. 1991). Evidence of oscillatory flow and bedding isotropy are the most crucial elements for differentiating between storm deposits and turbidites/antidunes and can be identified by accurate interpretation of HCS, SCS, wave-ripple character, and isotropic truncation of laminae within cross-bedded sedimentary structures.

3.3 Deep-Water Turbidites

Criteria for turbidites from bottom to top includes; fining upward graded interval. Sometimes gravel and sand occur in the lowest interval (Ta); lower interval of parallel

lamination (Tb) composed mainly of coarse-grained parallel lamination, although grading sometimes occurs; interval of current ripple lamination (Tc) with ripples no larger than 5 cm in height and 20 cm in length; distinct foreset lamination often is preserved. The contact between the Tb and Tc interval often is very apparent; upper level of parallel lamination composed of very fine sand to silty shale (Td). The contact between Tc and Td also is very distinct; Shaley interval (Te) with no visible sedimentary structures. A complete Ta-Te sequence is rare and most common turbidite deposits occur as incomplete sequences (Bouma 1962).

3.4 Wave-Modified Turbidites

Shallow-water turbidites deposited above SWB were documented in several cases (Bartolini et al. 1975, Cacchione and Drake 1990, Higgs 1990, 2014, Myrow and Southard 1996, Myrow et al 2002, Lamb et al. 2008). Shallow-water turbidites also are known as ‘wave-modified turbidites’ or ‘hyperpycnites’ (Higgs 1990, 2014, Myrow and Southard 1996, Myrow et al. 2002). These marine deposits occur when storms discharge dense sediment-rich river water into the ocean. These flows are driven by excess-weight forces and create deltas above SWB that can be modified by combined flows. Wave-modified turbidites can be identified by multiple criteria; (i) well-graded Bouma-like sequences; (ii) well-developed flutes; (iii) thick divisions of climbing ripple lamination; and (iv) and asymmetric folds and abundant convolute bedding (Myrow et al. 2002, Lamb et al. 2008). Wave- modified turbidites differ from deep-water turbidites in that

turbulence required to maintain hyperpycnal flows partially comes from storm waves and is not autosuspending in a purely density-driven flow.

3.5 Study Area Description

Two canyons and several road outcrops served as study sites for this thesis (Figure 1). Lozier Canyon, located in west Texas in Val Verde and Terrell Counties, terminates at the Rio Grande River. Antonio Creek terminates into Lozier Canyon, approximately four miles north of the Texas-Mexico border. Road-side and Osman Canyon outcrops are located along Texas Highway 90, east of Lozier Canyon. Lozier Canyon contains a complete vertical succession of the entire Eagle Ford Formation on multiple well-exposed outcrop faces. Lozier Canyon also serves as a valuable study site because Facies A and the contact with the underlying Buda Formation can be accessed at multiple locations along a 6-mile stretch of the canyon. Antonio Creek has less continuous vertical exposure, but provides access to bedding exposures of Facies A (Figure). Road outcrops along Texas Highway 90 are located approximately ten miles from Lozier Canyon and provide several exposures of Facies A at multiple locations, including Osman Canyon.

3.6 LiDAR

Light Detection and Ranging (LiDAR) scanning is useful for many aspects within the field of geology, most commonly for airborne surface fault mapping over a large area (Buckley et al. 2013). LiDAR also was used to differentiate between lithology using algorithms to increase the intensity variations between separate units with different physical and chemical characteristics (Jones et al. 2009; Buckley et al. 2013). This particular study uses a Leica C10 terrestrial LiDAR to measure the variation in ripple height across the faces of outcrops of Facies A in Lozier Canyon and Antonio Creek. Once the face of an outcrop is scanned, the three-dimensional mesh of data was uploaded to Cyclone® 8.0 software where each individual ripple can be measured across the outcrop.

4. METHODOLOGY

4.1 Outcrop Sampling and Data Collection

The primary aim of this study is to use observations and measurements of sedimentary structures to help determine the depositional environment of Facies A (Figure 5). Symmetry measurements were taken from three-dimensionally exposed ripples and samples were taken of samples with visible cross-bedding in Facies A (Figure 6). A secondary side-objective of this study is to determine the usefulness of LiDAR in outcrop studies.

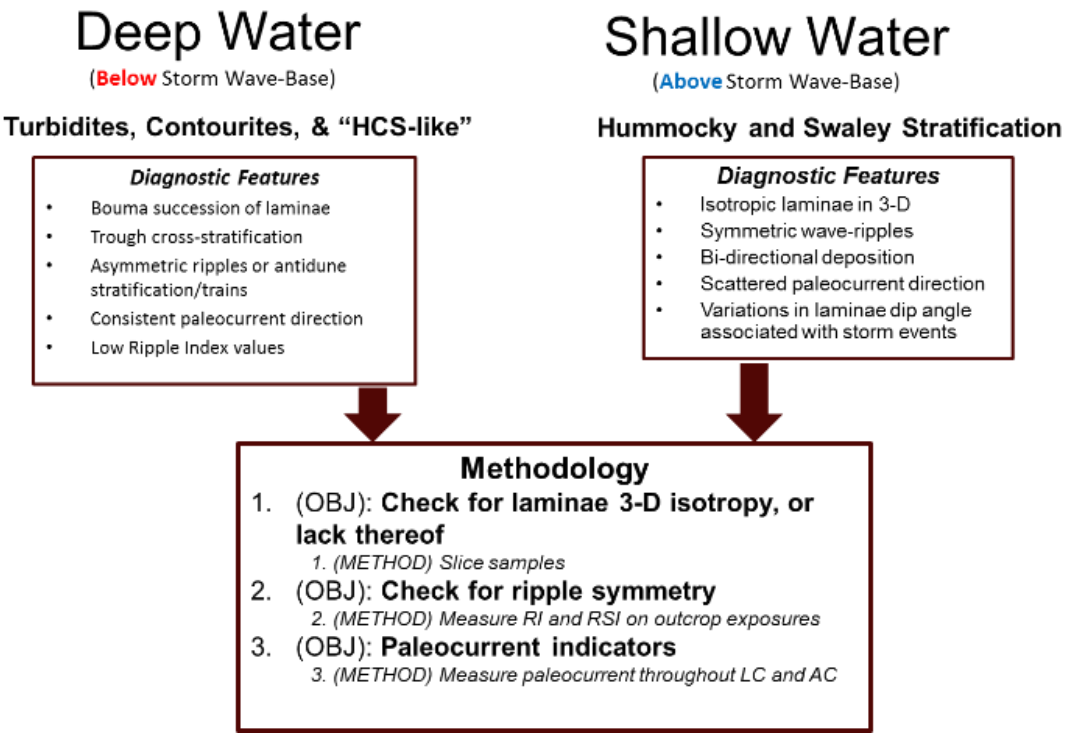

Figure 5. Step-by-step methodology. Used to determine whether Facies A was deposited above or below SWB.

Figure 6. Cross bedded grainstone bed. These beds frequently have three-dimensional exposure at Facies A at sampling location LC1.

Skeletal grainstone beds with observable cross-bedding in Facies A were sampled from multiple locations in Lozier Canyon and Antonio Creek (Figure 1). Before being removed, the samples were marked with their location, sample number, and arrow indicating which direction is up. Relatively large samples were selected so that a larger and more continuous suite of sedimentary features can be observed in each sample. Each grainstone sample was approximately 0.5 m (L) x 0.5 m (W) x 0.25 m (H). The samples were returned to the laboratory at Texas A&M University where they were cut into quarters using a large oil-based saw (Figure 7).

Figure 7. Oil-based rock-saw. Used for cutting clean, well-polished faces on rock samples from the field.

Because the cut from an oil-based saw is smooth, polishing the freshly cut rock face was not necessary in order to see well-defined laminations on the freshly cut surface. Most cuts were made 90° to each other to show isotropy and changes in 3-D geometry within the sample. Some extra cuts were made through the ripple crest of each sample to determine if laminations have similar geometry and truncations in all directions. Cuts revealed faces with flat laminations, whereas others have a large range of cross-bedding, truncations, and scour and drape features. The faces with the widest variety of sedimentary structures were photographed normal to the rock face.

Photographs of freshly cut faces 90° to each other were uploaded into Adobe Illustrator® where they were cropped, re-scaled, and meshed together to show a seamless image of laminae forms and truncation surfaces in three-dimensions. The meshed images were traced to accentuate bedding characteristics and make truncations more apparent. This process was used to demonstrate how beds truncate in three dimensions and allows us to observe small-scale sedimentary features that are not visible on weathered surfaces. LiDAR data was also taken for this study, but did not prove useful in making small-scale measurements of the face of the outcrop.

Ripple index (RI) measurements were taken by measuring the height of the ripple and the distance from trough to trough with a tape measure (Reineck and Singh 1975, Collinson et al. 2006). Ripple symmetry index (RSI) measurements were taken by measuring the length from the crest to the trough of the stoss side, then from the crest to the leeward side (Figure 8). Measurements for ripple symmetry were only taken on samples with 3-D exposure.

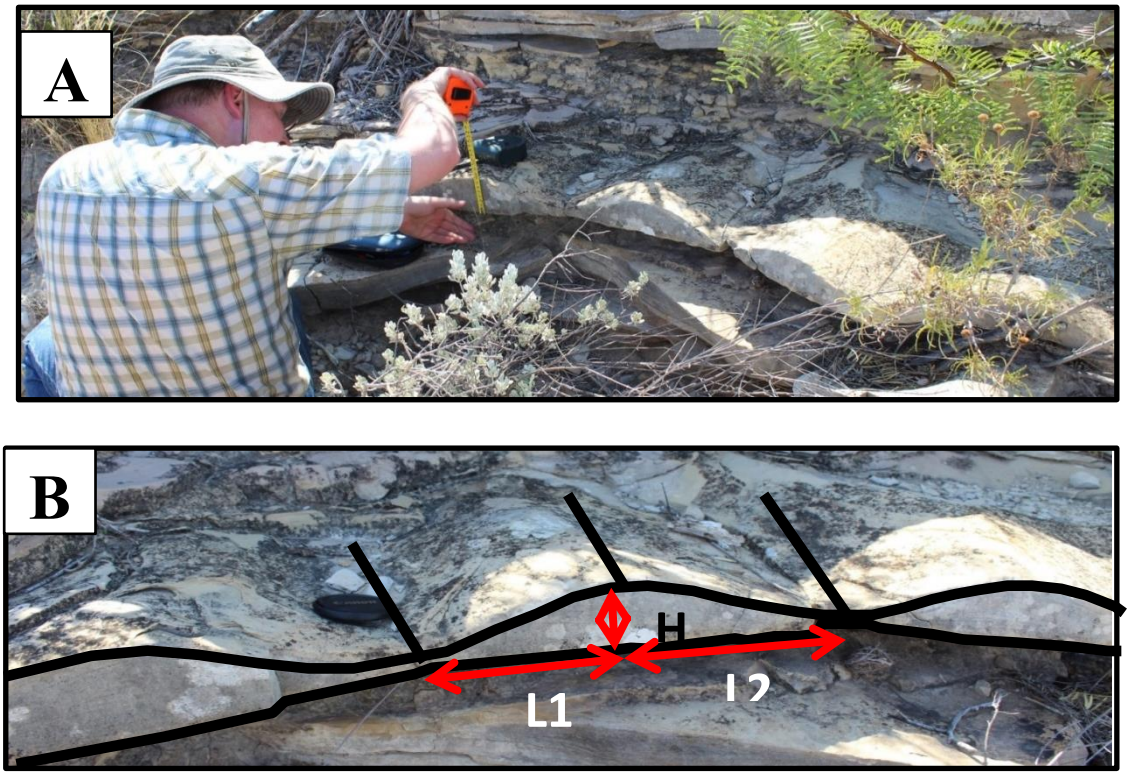

Figure 8. Ripple measurements methodology. (A) Tape measure was used to measure ripple dimensions. Field assistance was provided by Matthew Wehner (in photo). (B) Methodology of taking ripple measurements. The wavelength and amplitude of each ripple was measured with a tape measure. Lengths from the trough to crest (L1, L2) were measured on both sides of ripples to acquire symmetry data.

4.2 LiDAR Scans

A secondary objective of this study is to evaluate the usefulness of LiDAR for the observation and description of 3D sedimentary structures. The purpose of LiDAR ing for this project is to create high resolution 3D images upon which quantitative measurements of sedimentary structures and bed thickness variations on a centimeter-millimeter scale can be made. For this study a green laser Leica ScanStation C10 LiDAR

device was primarily used for surveying and has a high-definition range of up to 300 meters. As the LiDAR device scans the outcrop face, data points are recorded in 3 dimensions (Kurz et al. 2009, 2012; Buckley et al. 2013). From the same location, the 3D data set can be stitched over a high- resolution image of the outcrop face that is simultaneously recorded by the LiDAR device, creating a 3D projection of the outcrop that can be viewed and manipulated in Cyclone®. LiDAR images were taken of portions of Facies A that showed measurable ripples and sedimentary structures. Each scan was taken over an outcrop face approximately 25ft wide and 15ft tall. The scanner was set up ~15 meters from the outcrop face for each scan. After scanning the outcrop, LiDAR data were uploaded into Cyclone® where the ripple heights and wavelengths were measured using the "distance point-to-point" tool.

5. RESULTS

5.1 Facies A Outcrop- Lozier Canyon

Foraminiferal grainstone and packstone beds in Facies A commonly are <15 cm thick and often are discontinuous and pinch out over a length of 9 meters, though thicker laterally continuous beds occur (Figure 9). Thickness of each grainstone bed varies laterally and can pinch out and re-appear in the same lateral section. Many grainstone/packstone beds are amalgamated containing one or more throughgoing truncation surfaces and multiple ripple structures. Grainstone/packstone beds are separated from one another by an organic-rich shale layer that normally does not exceed 10 cm in thickness or an occasional thin bentonite bed. Cross-bedded grainstone/packstone units thin up-section within Facies A. Grading is rare, but does occur in select samples. The geometry and bedding of grainstone/packstone beds in Facies A in Lozier Canyon, Antonio Creek, and Osman Canyon can be separated into two categories; (i) Symmetric pinching and swelling amalgamated grainstones with parallel laminations and cross bedding present within each layer and; (ii) relatively flat-lying thicker beds ~10-15 cm thick that are laterally continuous and do not show 3-D laminae at the outcrop scale and commonly consists of parallel laminations. Type (i) beds can be concave up, concave down, or symmetric at the outcrop.

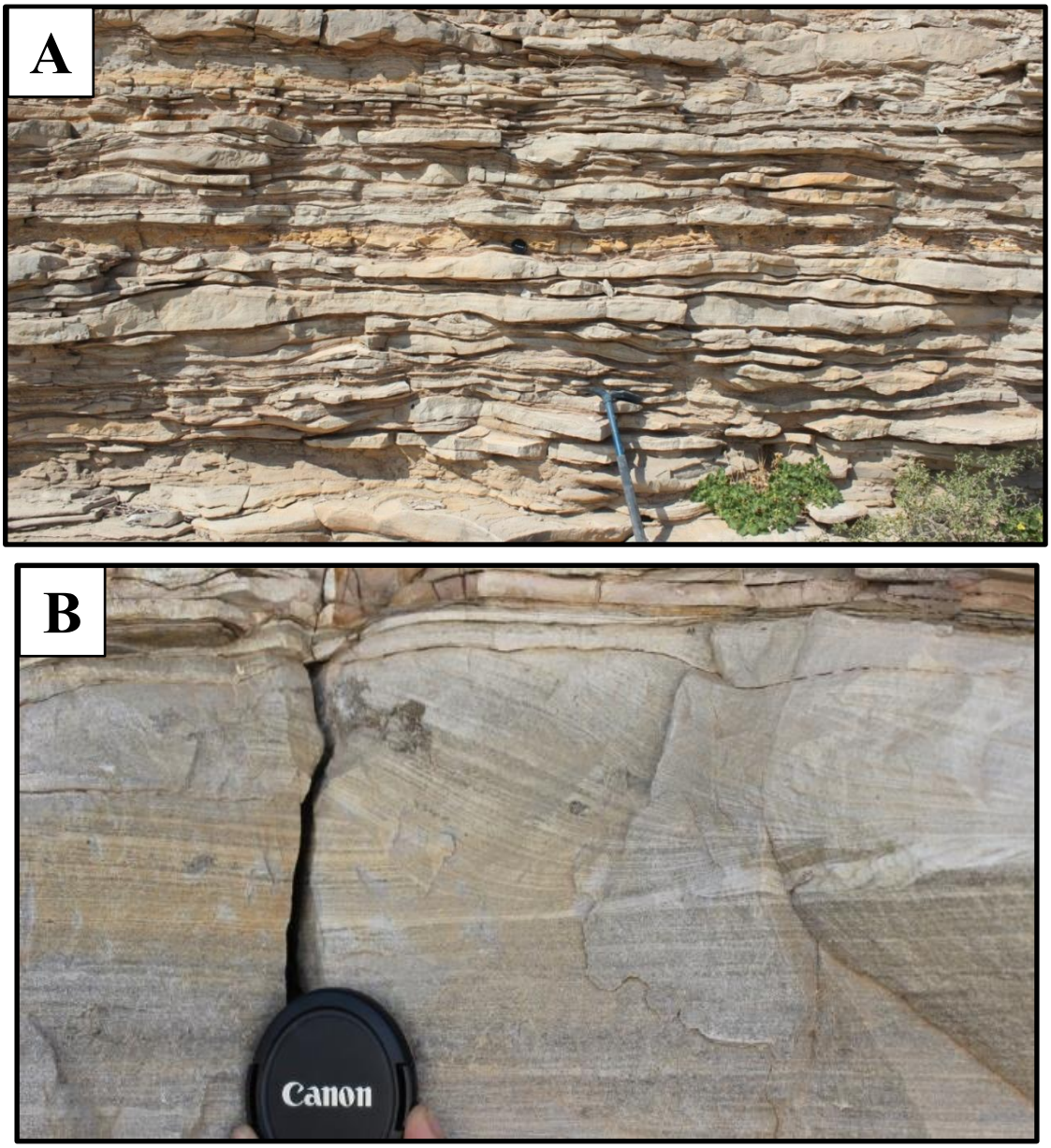

Figure 9. Sample location LC1 and LC 2. (A) Visible change in grainstone thickness and lateral continuity occurs across the face of the outcrop. (B) Scouring into parallel laminated beds. (C) Amalgamated grainstone beds.

Figure 9 Continued.

Type (i) beds can also have a pinched-out lens shape where the unit thickens and thins over a very short distance (~10 cm) and may pinch out and reappear as a single lens or continuous bed further across the unit. These beds have erosive and irregular bases. The dip of laminae within type (i) beds ranges from 10°-31° (Figure 9c). Steeply dipping laminae commonly cut down into underlying layers of parallel laminations. This unit (i) is most-likely to be referred to as a pinch-and-swell bed because of the way each lens is connected by a thinning unit that laterally expands into an adjacent lens within the same bed. Laminae in these units are both concordant and discordant with respect to the beds external geometry. Dips of laminae in these samples

can be as steep as 25°. Flat lying type (ii) beds sometimes have complex internal laminae that are discordant with the 3-D geometry of the sample. Cross bedding in type (ii) samples commonly occurs in multiple sequences of downlap, scour and drape features, with parallel laminations at the upper and lower bounds of the sample (Figure 10).

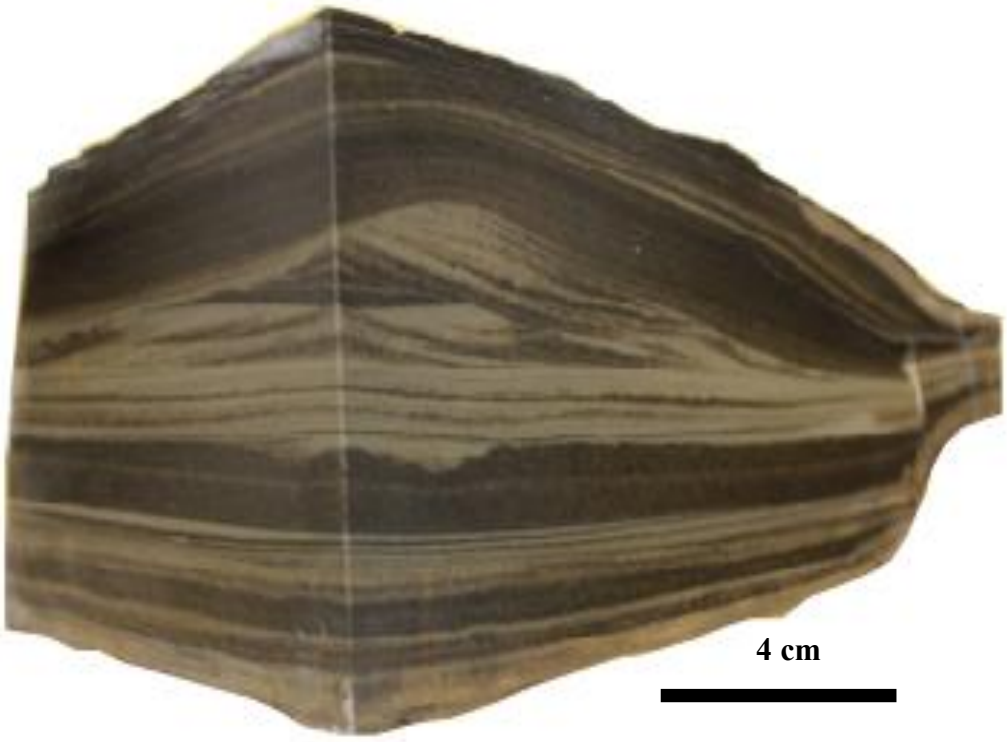

Figure 10. 90° cut sample from LC1-14. Cuts were made using an oil-based rock saw. Parallel lamination on upper and lower bounds. Erosional scoured surface below cross-bedded zone. Cross-bedding has mound shape and laminae dip isotropically in all directions.

5.2 Domal 3-D Exposures

Three-dimensional low-relief domal bedforms are exposed in a gully in Lozier Canyon close to Highway 90 (Figure 11). Erosion of the overlying strata made it possible to view a large area of the beds upper surface. The low-relief domal bedforms have an average wave height of 2.5 cm and wavelength of 14-20 cm producing an RI~8. The mounds have a slightly elliptical shape and concordant laminae that dip at a low angle when observed from the side.

5.3 Ripple Index, Symmetry, and Paleocurrent Measurements

Measurements of 2-D ripple amplitude, wavelength, and symmetry (Figure 8) were recorded at two locations in Lozier Canyon (LC1 and LC 2) (Figure 1). Ripples in Facies A are mostly symmetric with rounded crests and have an average ripple index (RI) of 6.0 and ripples symmetry index (RSI) of 1.23 (Figure 12).

Seven measurements of paleocurrent data were taken in Lozier Canyon and six were recorded in Antonio Creek (Figure 13). Measurements were taken from ripple crests and are scattered, having no regionally consistent measurement (Figure 7b). Scattered paleocurrent direction measurements around a compass are consistent with HCS paleocurrent directions (Bourgeois 1980, Brenchley 1989). Measuring paleocurrent on exposed fragments of domal upper surface, like those for HCS, would produce

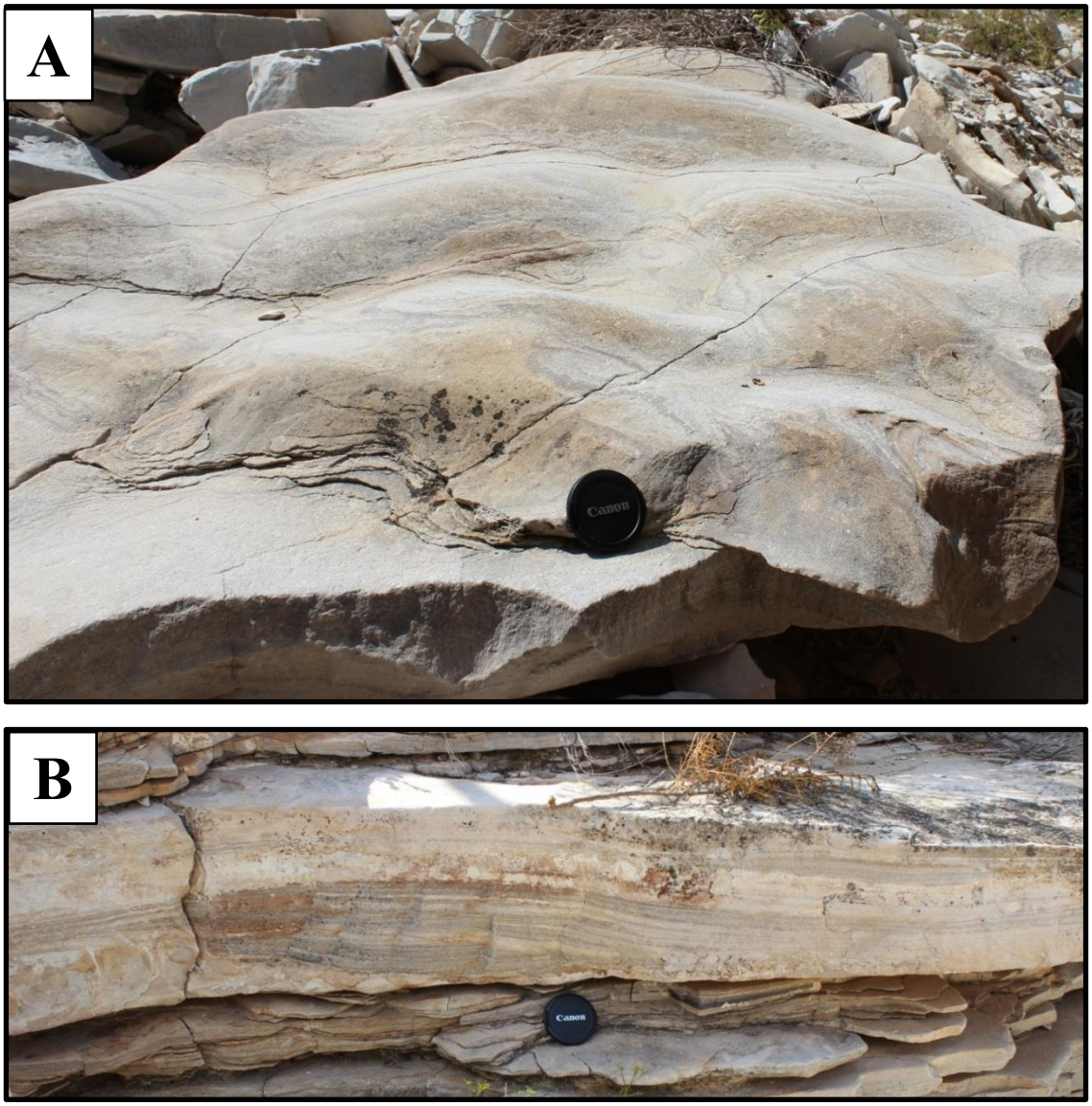

Figure 11. Domal features in Lozier canyon (LC1). (A) Domes resemble HCS upper surface and are arranged in a staggered orientation (B) Cross-sectional view of domal features. Cross-bedding is concordant with domal shapes and has low-angle stratification.

scattered data like those in Figure 13. HCS-like beds described by Mulder et al. (2009) have RI values that range from 12 to 25.

Ripples in Facies A have bi-directional downlap on both sides of ripples crests (Figure 14). Bidirectional downlap is a common feature at several locations throughout Lozier Canyon and Antonio Creek. Ripples with unidirectional deposition in Facies A have RI and RSI values that are indistinguishable from RI and RSI values of ripples with bidirectional deposition (R^2 = .042). The tops of all measured ripples are rounded. No wave ripples with peaked crests were observed in Lozier Canyon, Antonio Creek, or Osman Canyon.

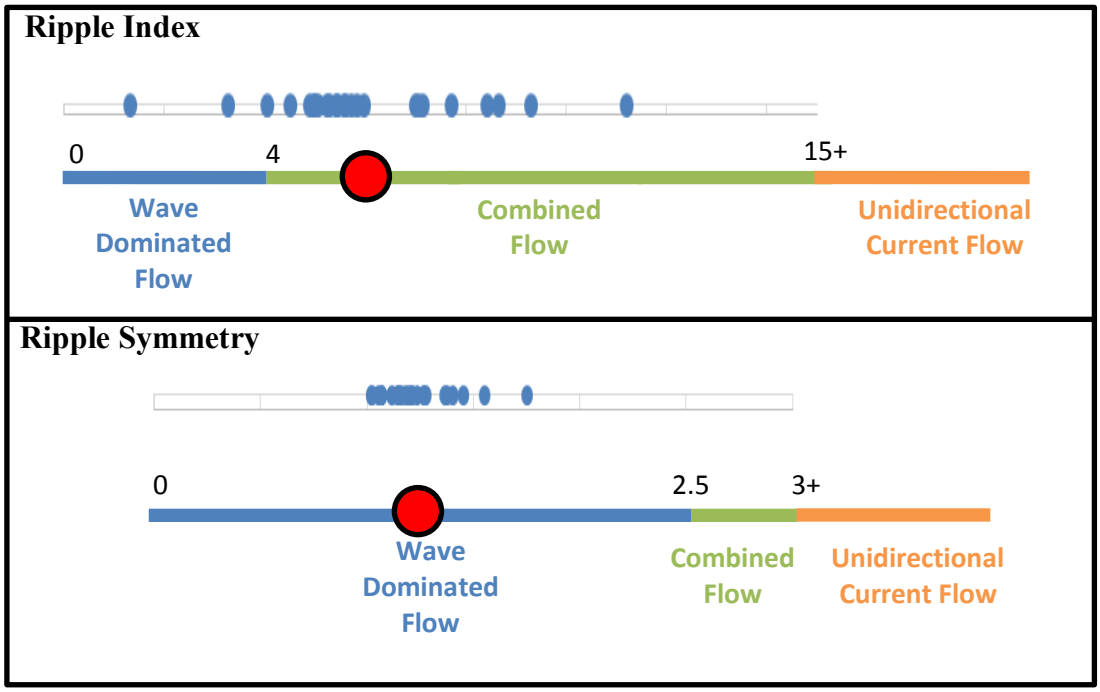

Figure 12. Ripple index and symmetry data. Blue dots are field data and the red dot is averaged data field. The data is plotted against standards for wave-dominated flow, combined flow, and unidirectional flow set by Reineck and Singh (1975), Collinson et al. (2006).

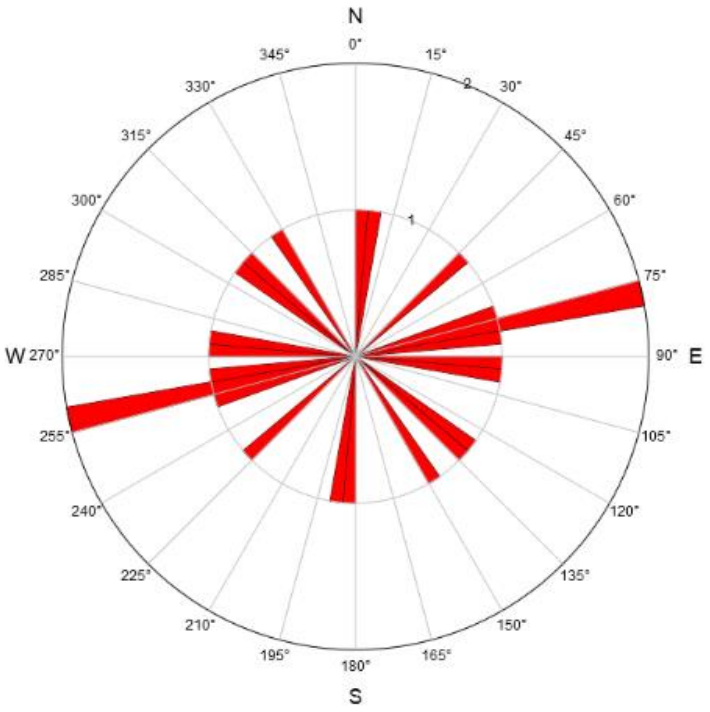

Figure 13. Rose diagram. Data represents paleocurrent measurements from Lozier Canyon (LC1 & LC2) and Antonio Creek. 13 measurements total.

Figure 14. Ripples with traced laminae. Laminae downlap on both sides of ripples crests. All of the observed ripples in Facies A have rounded crests like those in this figure above.

5.4 Contorted Beds

Contorted beds show a range of features in Facies A that were documented in Lozier Canyon, Antonio Creek, and Osman Canyon. The Osman Canyon outcrop is approximately 20 miles east of Lozier Canyon and Antonio Creek outcrops, which are relatively close to each other (Figure 1). Contorted beds also occur in other overlying facies within the Eagle Ford (Facies D and E) in Antonio Creek. However, Facies D and E are nodular and bioturbated, which makes distinction of features difficult.

The thickness, lateral variability, and location relative to the base of Facies A for the contorted beds in Lozier Canyon and Antonio Creek are very similar. Folded features in contorted beds at the Lozier Canyon and Antonio Creek outcrops indicate limited lateral transport. These beds are laterally discontinuous and can only be traced a few meters, with a maximum thickness of 0.6-1.5 m. The Lozier Canyon (LC1) outcrop contains two visible contorted beds that occur 1.5 and 4.5 meters from the base of Facies A and consist mostly of large clasts and deformed semi-continuous beds. More diverse features are exposed in Antonio Canyon. The contorted beds in Antonio Canyon have convolute bedding and diapiric fluid-escape structures (Figure 15).

The character of contorted beds in Osman Canyon is more laterally continuous and occurs at different heights above the Buda than those in Lozier Canyon and Antonio Creek. Osman Canyon has two distinct contorted beds that are continuous over a larger lateral area (> 60 m) and their thickness varies between 0.6 and 1.5 meters in thickness (Figure 2b). These contorted beds are located 0.9 m and 2.7 m from the base of Facies A.

Both of these contorted beds have deformed semi-continuous convolute bedding, load casts, and fluid escape structures.

Figure 15. Vertical fluid escape structures in Antonio Creek. Massive grainstone formed diapiric structures during upward fluid escape and deformation of the overlying ductile shale.

.

5.5 LiDAR Scans

LiDAR was unable to aid in this study because the required small scale and three-dimensional exposure of outcrop samples could not be achieved by this device. Bedding thickness measurements proved to be inaccurate in Cyclone when compared to physical measurements with a tape measure on the face of the outcrop.

6. DISCUSSION

The multiple, parallel slices of the largest Facies A samples provide insights about 3-D geometries that are difficult to ascertain on the outcrops. Cut samples allow observation of isotropic laminae, reactivation surfaces, variable laminae dip angles, large ripple wavelengths with symmetric rounded crests, and bidirectional downlap surfaces. These features suggest deposition in a storm-wave setting above SWB. Cross-bedded structures in Facies A contain sedimentary structures that most closely resemble small-scale HCS, SCS, and other storm deposit features, which suggest deposition under combined flow conditions. Ripple height measurements (Figure 12) are indicative of a depositional environment in which wave-influence is substantial (Reineck and Singh 1975, Collinson et al. 2006).

Sedimentary structures in Facies A are not identical to the description of HCS by Harms et al. (1975) because the observed sedimentary structures have short wavelengths on the decimeter scale, and laminae dips frequently exceed 10°. Sedimentary structures in Facies A do not indicate a turbidite system (Bouma 1962), because (Tc) cross-bedded intervals are often isotropic, bidirectional, and are frequently interbedded with fine muddy sediment.

6.1 Distinguishing Between HCS and Turbidite/Antidune Stratification

Cross-bedded structures in Facies A were interpreted as antidune stratified turbidites deposited in a deep-water environment below SWB (Ruppel et al. 2012). Observation of the internal geometry of samples for Facies A shows distinctions between storm-deposited HCS and deep-water turbidites/antidunes. Samples in Facies A have internal laminations with lateral truncations, wide array of laminae dip angles, and three-dimensional isotropy (Figure 16). These features are consistent with descriptions and experimentally reproduced HCS in a combined flow (Myrow and Southard 1991, Myrow 2002, Dumas and Arnott 2006, Perillo et al. 2014).

6.1.1 Internal Laminations

Cross-bedded samples in this study have laminae dip angles that vary from 10° to 30° (Figures 17). Normally, the dip angle for turbidites and contour currents is largely governed by the angle of repose (>30°). This study suggests that the large variations in dip angle for each respective sample are controlled by several factors such as: (i) variations in aggradation rate (Dumas and Arnott 2006); (ii) prolonged events of deposition and reworking (Perillo et al. 2014); (iii) and variations in unidirectional velocity for each respective depositional event (Dumas et al. 2005). Wave-tank experiments indicate that an increase in aggradation rate results in an average increase in dip of the leeward side of cross-laminae (Dumas and Arnott 2006). Flow duration and

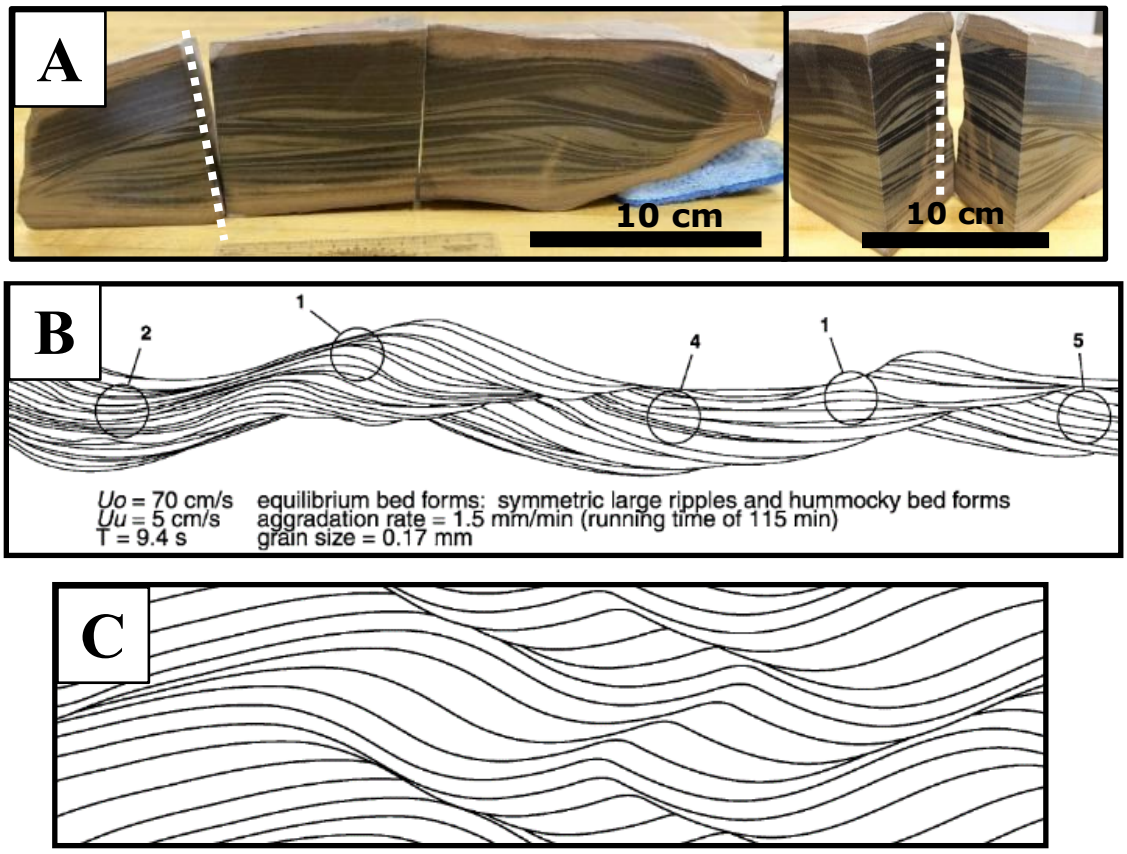

Figure 16. Structures produced in experiments (A) Multiple generations of scour and fill and swaley cross-stratification. A 90° cut was made through the plane marked with the dotted like to view truncation in three-dimensions. Swaley cross-stratification in this sample is compared to experimentally reproduced structures (b) and (c). (B) Wave-tank experiment. Experimentally produced swaley cross-stratification formed under oscillatory dominant combined flow, which closely resembles Facies A in Figure 16a. Modified figure from Dumas and Arnott (2006). (C) In the same series of experiments performed by Dumas and Arnott (2006), aggradation rate was increased , which caused an increase in preserved dip-angle of laminae. Produced Samples appear similar to those observed in Facies A. However, these structures lack a flat basal surface similar to structures in Facies A. Modified figure from Dumas and Arnott (2006).

velocity also are important factors that control the ability of a bedform to grow until it reaches maturity with respect to flow conditions (Perillo et al. 2014).

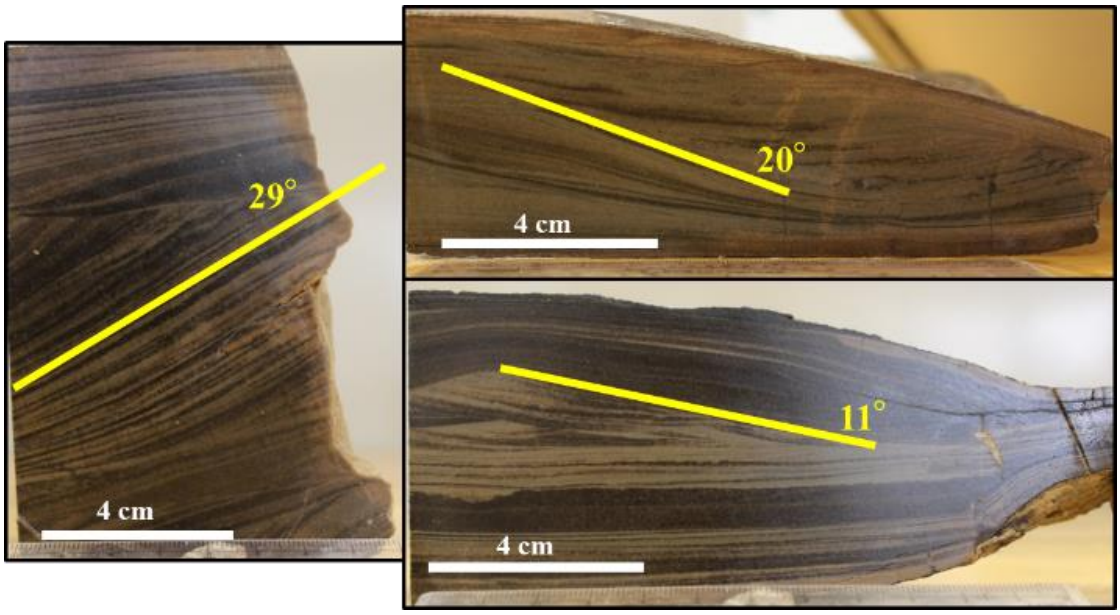

Figure 17. Cut samples from Lozier Canyon. This figure shows varying degrees of bedding dip angle.

Lateral truncations and truncation surfaces (Figure 18) are most likely the result of a brief change in flow direction, associated with oscillatory flow. This type of bedding character is highly unlikely in a high-velocity depositional setting that would cause antidune stratification (Rust and Gibling 1990). Antidune laminae are preserved on the stoss side of deposition, which indicates that this type of truncation (Figure 18) was not formed by antidune stratification (Simons and Richardson 1961, Middleton 1965, Rust and Gibling 1990). These truncations also are inconsistent with high-energy unidirectional flows associated with continuous trough cross-bedding deposition in turbidites because rapid density-driven flows have no method of reversing flow to cause such truncation surfaces.

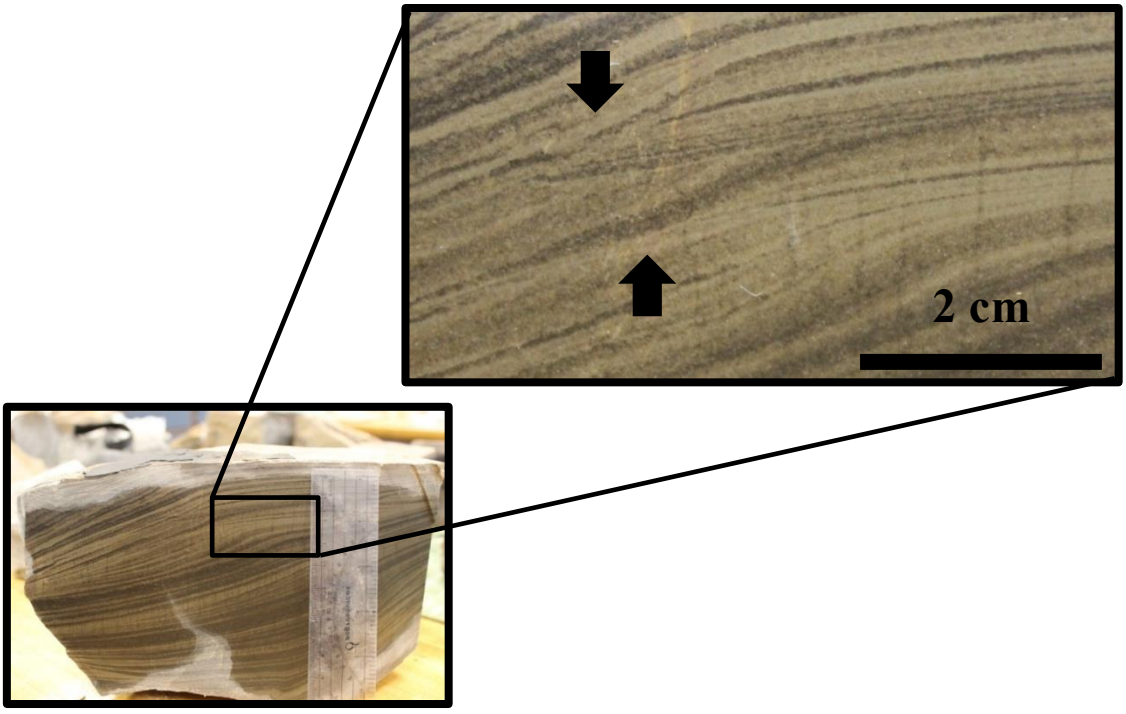

Figure 18. Truncation surfaces in Facies A. These are found in numerous samples from Lozier Canyon. Arrows identify two truncation surfaces that were formed during deposition.

6.1.2 Three-Dimensional Geometry and Isotropy

The most distinct differences between combined flow wave-dominated sedimentary structures and unidirectional current-flow structures are isotropic laminae that dip evenly across 360° and the presence of symmetric wave-ripples with bi-directional downlap. Isotropic laminae (Figure 4) are characterized by similar dip angle in all directions and are a distinct characteristic of HCS and SCS (Harms et al. 1975, Bourgeois 1980, Walker and Leckie 1982, Snedden et al. 1988, Brenchley 1989). Wave oscillation associated with storm events causes sediment to be draped over an irregularly scoured surface and moves sediment into circular mounds of HCS and SCS (Southard et al. 1990, Myrow and Southard 1996). Samples from Facies A have a wide variety of internal geometries, most of which have isotropic laminae and bundled foresets that truncate symmetrically across a 90° cut (Figure 19). Concave-up drape-like geometry is most common in SCS and is deposited in scoured troughs as the synform extension of antiform HCS beds into lower areas. In fact, synforms (SCS) are most commonly preserved from HCS beds, which is why they are so frequently mistaken for trough cross-stratification (Dott and Bourgeois 1982). The ability to see isotropic truncation of SCS in three-dimensions is inconsistent with trough cross-bedding described in Tc intervals of turbidite deposits and is at too high of an angle to be confused with 3-D antidunes. Short-lived energy dispersals from
the Kelvin-Helmholtz instability would not be capable of sustaining the required wave-energy to rework largely isotropic sedimentary structures like those in Facies A.

6.1.3 Domal 3-D Exposures

Three-dimensional low-relief domal bedforms in Lozier Canyon mounds have a slightly elliptical shape and concordant laminae that dip at a low angle when observed from the side, similar to HCS mounds (Harms et al. 1975). The mounds are organized in a staggered orientation, which is consistent with the domal three-dimensional upper surface of HCS bedding. Mound organization like this is inconsistent with the hypothesis that cross-bedded structures in Facies A formed by antidunes (Ruppel et al. 2012). Wave tank experiments indicate that antidune stratification produces laterally continuous trains, or crest axes, in well-ordered successions (Middleton 1965, Barwis and Hayes 1985, Rust and Gibling 1990, Alexander et al. 2001, Cartigny et al. 2014). These uniquely exposed bedforms in Lozier Canyon are interpreted as combined flow HCS mounds and further indicate deposition above SWB.

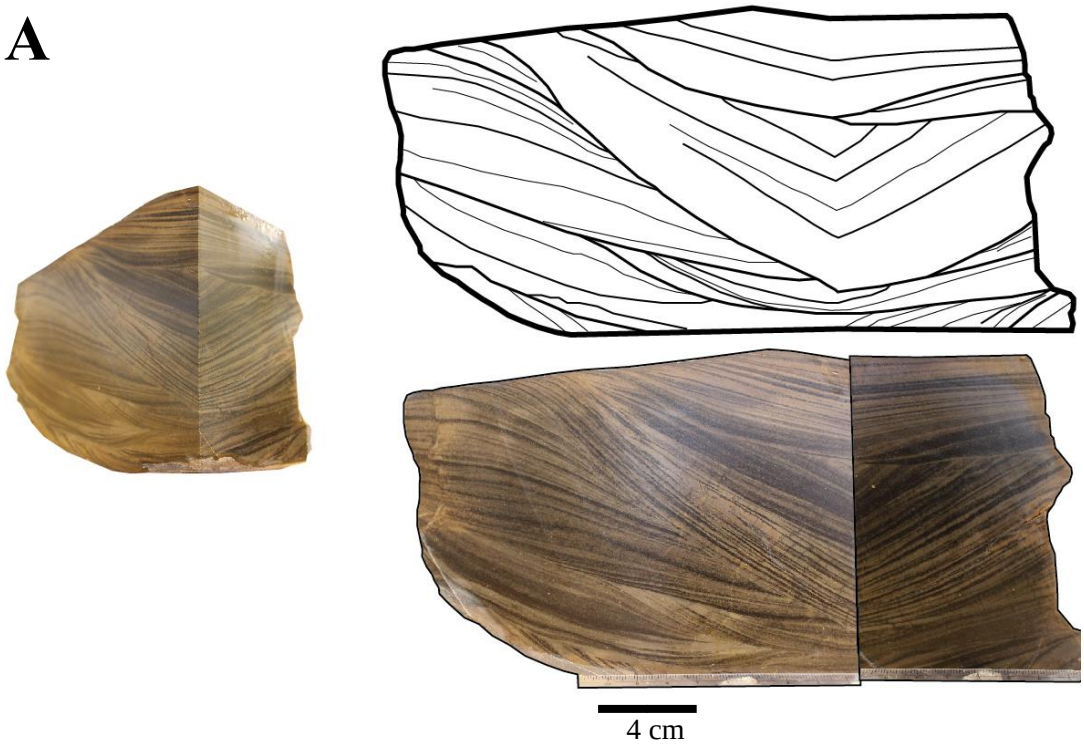

Figure 19. Samples were cut at right angles to reveal bedding features in 3D. (A) Sample LC1-9. has concave-up bowl-like shape in three-dimensions and has bundled foresets that indicate multiple generations of bundled foresets. Laminae that dip evenly across a right angle indicate isotropy. (B) Sample LC1-1 shows laminae that dip evenly across a right angle, scoured basal surfaces, and parallel laminae with low-angle stratification. (C) Sample LC1-4 has a mound-like shape in three-dimensions with laminae truncating evenly across 90°. A cross-bedded zone is bound by parallel laminations at the top and bottom of the sample. Scouring of the basal parallel laminations can be observed. Cross-bedding has a concave-up and concave-down shape in three-dimensions. (D) Sample LC2-1 has cross-bedded laminae have a domal concave-down shape and dip evenly across a right angle. Dip angle also varies laterally in this sample, indicating change in flow velocity and/or sediment supply.

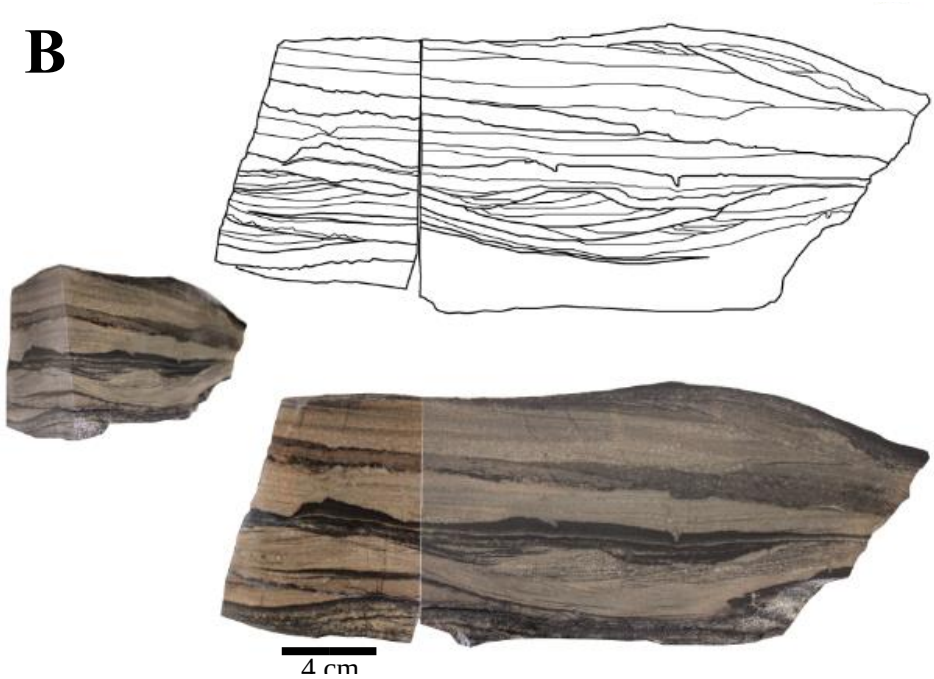

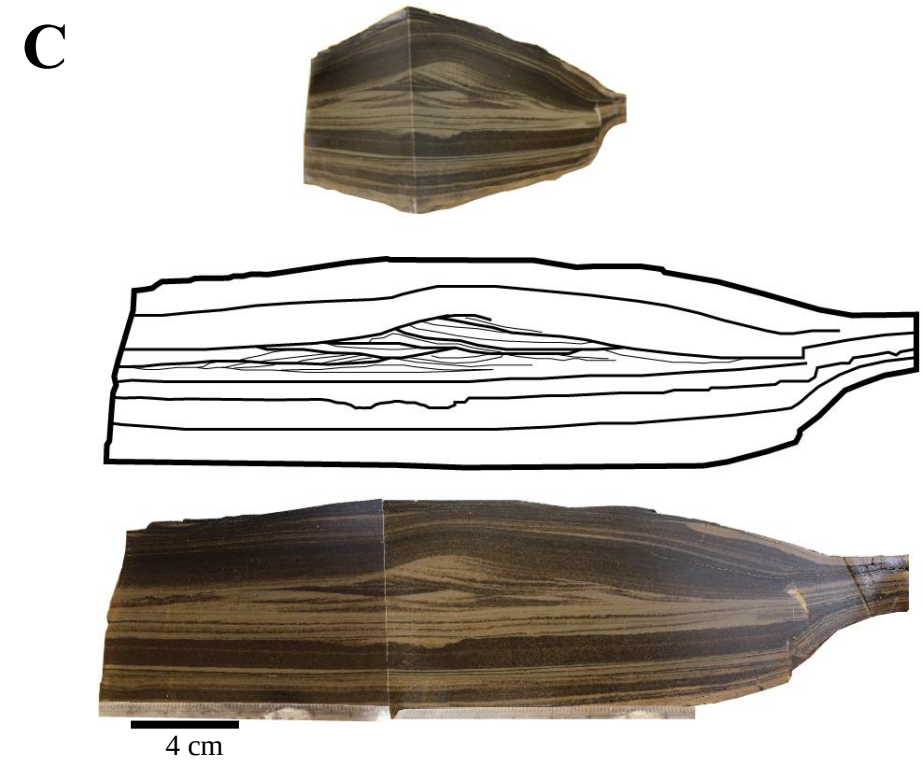

Figure 19 Continued.

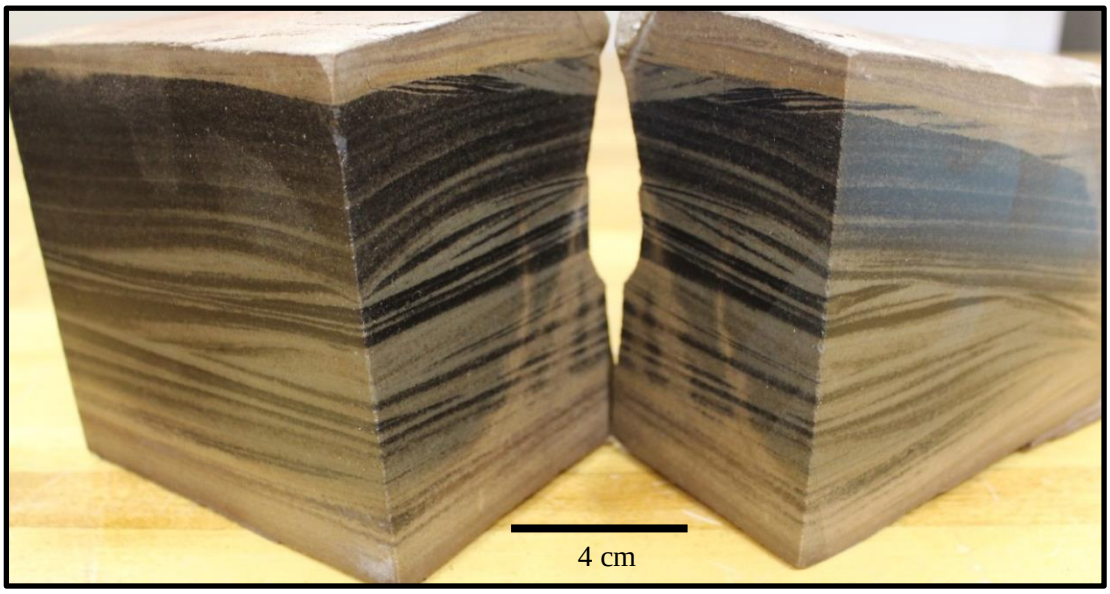

Figure 19 Continued.

6.1.4 Lineation and Paleocurrent indicators

Lineations and clear paleocurrent indicators are common in turbidite and antidune stratification where strong unidirectional currents are responsible for deposition (Middleton 1965, Anketell and Lovell 1976, Stow 1979, Rust and Gibling 1990, Alexander et al. 2001). Lineations in HCS are rare and are rarely documented (Duke 1985, 1987, Brenchley 1985). Similarly, no lineations were observed in Facies A. Because the laminae dip isotropically, acquiring paleoflow vectors was not possible on 3-D exposures of cross bedded samples. The lack of consistent paleoflow indicators suggests that Facies A was deposited in an environment where unidirectional flow was

dominated by strong oscillatory flow, preventing the generation of lineations or consistent unidirectional trough cross-stratification.

6.2 Ripples

Ripples in Facies A do not occur in any particular sequence with respect to cross-bedded layers or layers of organic-rich mudstone. This being considered, the character of the ripple height, wavelength, and crest shape can still indicate whether or not the depositional environment was influenced by oscillatory motion above SWB.

6.2.1 Symmetry

Ripples in Lozier Canyon and Antonio Creek are strongly symmetric with unidirectional and bidirectional downlap. Ripples with downlap on both sides of the ripple crests indicate influence of oscillatory wave-motion (Figure 14).

Symmetric bedforms are important in recognizing wave-influence in an environment, but does not negate the possibility of asymmetric bedforms to form in wave-influenced environments as well. Asymmetric bedforms, similar to trough cross-stratification, were reproduced in wave-tank experiments still being primarily influenced by oscillatory wave-motion in combined flow (Dumas and Arnott 2006, Perillo et al. 2014). Asymmetric HCS and ripple geometry often are attributed to an increase in unidirectional current velocity in combined flow and have a preferred direction of

asymmetry towards the down-flow direction (Allen 1982, Nottvedt and Kreisa 1987, Myrow and Southard 1991). During storm surges, strong backflow currents flow seaward and can transport large quantities of sediment across a shelf, thus skewing the shape of deposited sedimentary structures and causing asymmetry as well as amalgamation (Myrow and Southard 1996, Dumas and Arnott 2006).

6.2.2 Ripple Crests

Ripples in Facies A do not exhibit the characteristic peaked-crest shape associated with wave oscillation in a shallow-water environment. Instead, the ripples in Facies A most commonly have relatively large wavelengths and rounded crests. Ripples with rounded crests were frequently observed and reproduced in combined flow settling (Harms 1969, Reineck and Singh 1980, Arnott and Southard 1990, Dumas et al. 2005). The hydrodynamic conditions required to create ripples with round crests suggests that deposition occurred during a storm event (Yokokawa 1995, Myrow and Southard 1996, Lamb et al. 2008, Myrow et al. 2008, Yamagichi and Sekigichi 2010). The presence of ripples with round crests similar to storm ripples is further evidence that Facies A was deposited above SWB. The presence of storm-related ripples and the lack of peaked crests suggests that the depositional environment was between fair-wave base (FWB) and SWB.

6.2.3 Measured Data

Mound-like geometry of HCS and SCS makes accurate paleocurrent measurements very difficult (Bourgeois 1980, Brenchley 1989). However, wave ripples often form conjunction with HCS and SCS in tempestite deposits (Aigner 1982, Dott and Bourgeois 1982). The data from wave ripples in Facies A suggests the flow regime was symmetric. Generally, lower RI values (< 4) and RSI's (< 2.5) represent wave-dominated flow, and higher RI's (> 15) and RSI's (> 3) represent strong unidirectional flow (Reineck and Singh 1975 p. 35, Collinson et al. 2006 p. 76). Combined flows have RI's between 4 and 15. Average RI (6) and RSI (1.23) for Facies A indicate that ripples are strongly symmetric and formed in a combined flow regime.

6.3 Implications for Depositional Environment

6.3.1 Comparison to structures in the Basque Flysch (Mulder et al. 2009)

The suggestion that cross-bedded features in Facies A were deposited in a similar setting as HCS-like antidune stratified turbidites in the Basque Flysch (Ruppel et al. 2012), described by Mulder et al. (2009), neglects several crucial factors that should be included when interpreting sedimentary structures and their depositional environment; (i) The Eagle Ford Group was deposited on the Comanche Platform carbonate shelf, which bears little resemblance to the bathymetry of the Saint-Jean-de-Luz intracratonic

basin (1000-1500 m) where the Basque Flysch was deposited; (ii) The Basque Flysch outcrop is 3,000 m thick, whereas the Eagle Ford is only 52 m thick in Lozier Canyon; (iii) Cross-bedded structures described as HCS-like don't resemble strong three-dimensional resemblance to the cross-bedded structures in Facies A (Mulder et al. 2009). In contrast to Facies A, laminae in the Basque Flysch have: (i) more lateral continuity; (ii) gently dipping laminae (< 15°) and lack ripples; (iii) frequent antidune-like stratification with a higher RI (h/l ratio); (iv) clear, unidirectional paleoflow indicators; and (v) contains no sharp breaks in grain size or scoured basal surfaces.

The hydrodynamic conditions required to deposit the structures in the Basque Flysch occur under a very narrow range of parameters that are highly unlikely to occur on a gently-dipping carbonate shelf in the WIS for Facies A, because a steeply dipping slope is required to create a K-H instability. To generate turbidites that can be reworked by upslope antidune stratification caused by the K-H instability, a high-angle paleoslope and large amount of sediment supply are required (Quin 2011). Laminae dip directions frequently reverse throughout outcrops of Facies A in Lozier Canyon and Antonio Creek (Figure 20), this type of flow reversal is unlikely on a slope that was steep enough to produce a turbidity current. One could argue up-slope wave-migration from the Kelvin-Helmholtz instability created these flow reversals. However, the energy required from such a wave would have to be sustained for a long enough time period and with enough energy to deposit high-angle cross bedding up slope, which is not hydrodynamically plausible. Instead, this study suggests that changes in dip direction are simply the result of oscillatory wave-motion in a combined flow above SWB.

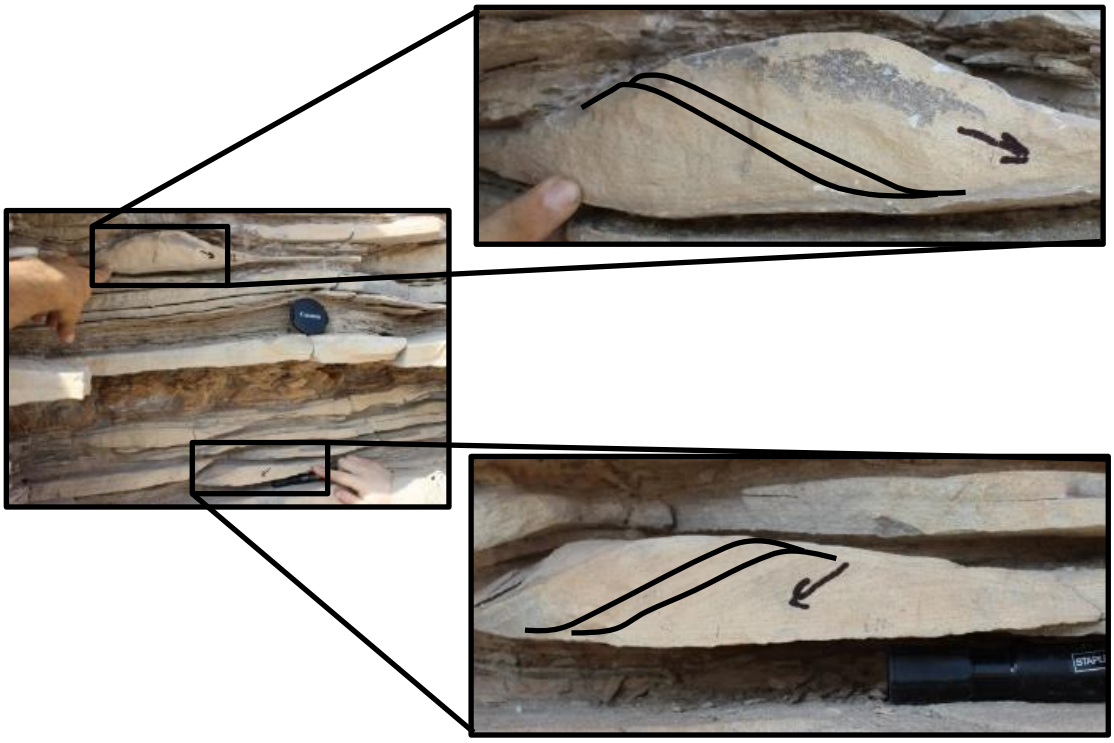

Figure 20. Change in dip direction within a small vertical section (Lozier Canyon).

6.3.2 Wave-Modified Turbidites (Hyperpycnites)

Interpretation of sedimentary structures in Facies A as HCS and SCS places the depositional environment above SWB in a shallow shelf setting in which storms frequently deposited and reworked sediment. The possibility of generating turbidity flows from excess-weight forces in a gently dipping shelfal setting is unlikely.

A relatively steep slope is required to achieve a self-sustaining turbidity current that can entrain large volumes of sediment (Swift 1986, Bangold 1962, Parker 1982). The most viable explanation for a density-driven turbidite-like deposits on a shelf would be hyperpycnites, or 'wave-modified turbidites' (Higgs 1990, 2014, Myrow and Southard 1996, Myrow et al. 2002, Luca and Basilici 2013). These fluvial deposits occur when storms discharge cool, dense, sediment-rich river water into the ocean, creating deltas above SWB that can be modified by combined flows. Common characteristics of hyperpycnites are; (i) well-graded Bouma-like sequences; (ii) well developed flutes; (iii) thick divisions of climbing ripple lamination; and (iv) and asymmetric folds and abundant convolute bedding (Myrow et al. 2002, Lamb et al. 2008). Cross-bedded structures in Facies A contain few of the criteria necessary for wave-modified turbidites: (i) grading in Facies A is rare, with the exception of tempestite storm event beds; (ii) facies A has no flute casts and few paleocurrent indicators ; and (iii) structures in Facies A also show no indication of supercritical climbing current ripples associated with density-induced flow (Myrow and Southard 1996).

7. CONCLUSIONS

The cross-bedded structures in Facies A outcrops of the Eagle Ford Group in west Texas are interpreted as small-scale HCS and SCS end-members associated with storm deposition above SWB on a shallow-water low-angle carbonate ramp. Bedforms were deposited by combined flows with strong unidirectional currents and oscillatory wave-motion. Sedimentary features in Facies A exhibit characteristics that are indicative of storm deposits, such as: (i) laminae that drape in all directions in a mound-like geometry similar to HCS and SCS; (ii) evidence for oscillatory flow, such as symmetric round-crest ripples with bi-directional deposition on both sides of ripple crests; (iii) a wide variety of bedform geometry and laminae dip angle, which are associated with variations in storm intensity, duration, sediment supply, and relative sea level; (iv) frequently amalgamated and node-shaped shaped bedding, consistent with sediment transported across a shelf in a storm-dominated environment; (v) and a low RI and RSI of measured ripples that is consistent with formation in a wave-dominated combined flow regime above SBW.

LiDAR scans of Facies A proved not to be useful for the purposes of this study.

REFERENCES

Adkins, W., and Lozo, F., 1951, Stratigraphy of the Woodbine and Eagle Ford, Waco area, Texas. Dallas Petroleum Geologists, p. 101-161

Aigner, T., 1982, Calcareous tempestites: storm-dominated stratification in Upper Muschelkalk limestones (Middle Trias, SW-Germany). p. 180-198, Springer Berlin Heidelberg.

Aigner, T., 1985, An ancient storm storm depositional system: Dynamic stratigraphy of intracratonic carbonates, upper muschelkalk (middle triassic), south-german basin, p. 51-158, Springer Berlin Heidelberg.

Allen, J., 1982, Sedimentary Structures: their character and physical basis. Elsevier, Amsterdam. v. 1

Alexander, J., Bridge, J., Cheel, R., and Leclair, S., 2001, Bedforms and associated sedimentary structures formed under supercritical water flows over aggrading sand beds. Sedimentology, v. 48, no. 1, p. 133-152

Anketell, J., and Lovell, J., 1976, Upper Llandoverian Grogal Sandstones and Aberystwyth Grits in the New Quay area, Central Wales: a possible upwards transition from contourites to turbidites. Geological Journal, v. 11, no. 2, p. 101-108

Arnott, R., and Southard, J., 1990, Exploratory flow-duct experiments on combined-flow bed configurations, and some implications for interpreting storm-event stratification. Journal of Sedimentary Research, v. 60, no. 2

Bagnold, R., 1962, Auto-suspension of transported sediment; turbidity currents. Proceedings of the Royal Society of London. Series A, Mathematical and Physical Sciences, p. 315-319

Bartolini, Carlo, Berlato, S., and Bortolotti, V., 1975, Upper Miocene shallow-water turbidites from western Tuscany. Sedimentary Geology v. 14, no. 2, p. 77-122

Barwis, J., and Hayes, M., 1985, Antidunes on modern and ancient washover fans. Journal of Sedimentary Research, v. 55, no. 6

Bohacs, K., Lazar, and Demko, T., 2014, Parasequence types in shelfal mudstone strata—Quantitative observations of lithofacies and stacking patterns, and conceptual link to modern depositional regimes. Geology, v. 42, no. 2, p. 131-134

Bourgeois, J., 1980, A transgressive shelf sequence exhibiting hummocky stratification: the Cape Sebastian Sandstone (Upper Cretaceous), Southwestern Oregon: Journal of Sedimentary Petrology, v. 50, no. 3, p. 681-702

Bouma, A., 1962, Sedimentology of some flysch deposits- a graphic approach to interpretation, Elsevier, Amsterdam: Journal of Sedimentary Petrology, p.168

Bouma, A., 1972, Fossil contourites in lower Niesenflysch, Switzerland: Journal of Sedimentary Petrology, v. 42, no. 4, p. 917-921

Brackenridge, R., Stow, D. A. V., and Hernandez-Molina, F., 2011, Contourites within a deep-water sequence stratigraphic framework: Geo-Mar Lett, v. 31, p. 343-360

Brenchley, P., 1985, Storm-influenced sandstone beds. Modern Geology, v. 9, p. 369-396

Brenchley, P., 1989, Storm sedimentation: Geology Today, p.133-137

Buckley, S., Kurz, T., Howell, J., and Schneider, G., 2013, Terrestrial LiDAR and hyperspectral data fusion products for outcrop analysis: Computers and Geosciences, v. 54, p. 249-258

Cacchione, D., and Drake, D., 1990, Shelf sediment transport: an overview with applications to the northern California continental shelf. In: The sea, v. 9, D. Hanes and B. LemiHauti, editors, Wiley and Son, New York, p. 729-773

Cartigny, M., Ventra, D., Postma, G., and Den Berg, J., 2014, Morphodynamics and sedimentary structures of bedforms under supercritical-flow conditions: New insights from flume experiments. Sedimentology, v. 61, no. 3, p. 712-748

Collinson, J., Mountey, N., Thompson, D., 2006, Sedimentary Structures, Third Edition, p.76

Christie-Blick, N., Von der Borch, C., DiBona,P., 1990, Working hypothesis for the origin of the Wanoka Canyons (Neoproterozoic), South Australia. Am. J. Sci. no. 290A, p. 295-332

Craft, J., and Bridge, J., 1987, Shallow-marine sedimentary processes in the Late DevonianCatskill Sea, New York State. Geological Society of America Bulletin, v. 98, no. 3, p. 338-355

Dawson, W. C., 2000, Shale microfacies: Eagle Ford Group North-Central Texas outcrops and subsurface equivalents: GCAGS, v. L, p. 607-621

Donovan, A., and Staerker, 2010, Sequence stratigraphy of the Eagle Ford (Boquillas) Formation in the subsurface of South Texas and outcrops of West Texas: GCAGS Journal, v. 60, p. 861-899

Donovan, A., Staerker, S., Pramudito, A., Li, W., Corbett, M., Lowery, C., Romero, A. M., and Gardner, R., 2012, The Eagle Ford outcrops of West Texas: A laboratory for understanding heterogeneities within unconventional mudstone reservoirs: GCAGS Journal, v. 1, p.162-185

Dott, R., and Bourgeois, J., 1982, Hummocky cross-stratification: significance of its variable bedding equences. Bulletin of the Geological Society of America, v. 93, p. 663-680

Duan, T., Gao, Z., Zeng, Y., and Stow, D., 1993, A fossil carbonate contourite drift on the Lower Ordovician palaeocontinental margin of the middle Yangtze Terrane, juixi, northern Hunan, southern China: Sedimentary Geology, v. 82, p. 271-284

Duke, W., 1985, Hummocky cross-stratification, tropical hurricanes, and intense winter storms. Sedimentology, v. 32, no. 2, p. 167-194

Duke, W., 1987, REPLY Hummocky cross-stratification, tropical hurricanes, and intense winter storms. Sedimentology, v. 34, no. 2, p. 344-344

Duke, W., 1990, Geostrophic circulation or hallow marine turbidity currents? The dilemma or paleoflow patterns in storm influenced prograding systems: Journal of Sedimentary Petrology, v. 60, no. 6, p. 870-883

Duke, W., Arnott, W., Cheel, R., 1991, Shelf sandstones and hummocky cross stratification: New insight on a stormy debate. Geology, v. 19, p. 625-628

Dumas, S., Arnott, R., and Southard, J., 2005, Experiments on oscillatory-flow and combined-flow bed forms: implications for interpreting parts of the shallow-marine sedimentary record. Journal of Sedimentary research, v. 75, no. 3, p. 501-513

Dumas, S., and Arnott, R., 2006, Origin of hummocky and swaley cross-stratification—the controlling influence of unidirectional current strength and aggradation rate. Geology, v. 34, no. 12, p. 1073-1076

Einsele, G., Ricken, W., and Seilacher, A, 1991, Cycles and events in stratigraphy.

Freeman, V. L., 1961, Contact of Boquillas Flags and Austin Chalk in Val Verde and Terrell Counties, Texas: USGS, p. 105-107

Freeman, V. L., 1968, Geology of Comstock-Indian Wells area Val Verde, Terrell, and Brewster counties, Texas: USGS Professional paper, v. 594-K, p. 26

Gardner, R., Pope, M., Wehner, M., Donovan, A., 2013, Comparative stratigraphy of the Eagle Ford Group strata in Lozier Canyon and Antonio Creek, Terrell county, Texas: GCAGS, v. 2, p. 42-52

Greenwood, B., and Sherman, D., 1986, Hummocky cross-stratification in the surf zone. flow parameters and bedding genesis. Sedimentology, v. 33, p. 33-46

Hamblin, A., and Walker, R., 1979, Storm-dominated shallow marine deposits: the Fernie-Kootenay (Jurassic) transition, southern Rocky Mountains. Canadian Journal of Earth Sciences, v. 16, no. 9, p. 1673-1690

Harms, J., 1969, Hydraulic significance of some sand ripples. Geological Society of America Bulletin, v. 80, no. 3, p. 363-396

Harms, J., Southard, J., Spearing, D., and Walker, R., 1975, Depositional environments as interpreted from primary sedimentary structures and stratification sequences. SEPM Short Course, no. 2

Heezen, B. C., Hollister C. D., and Reddman, W. F., 1966, Shaping of the continental rise by deep geostrophic contour currents: Science, v. 152, p. 502-508

Higgs, R., 1990, Is there evidence for geostrophic currents preserved in the sedimentary record of the middle to inner shelf deposits: Discussion. Journal of Sedimentary Petrology, v. 60, p. 630-632

Higgs, R., 2011, Hummocky cross-stratification-like structures in deep-sea turbidites: Upper Cretaceous Basque basins (Western Pyrenees, France) by Mulder et al. (2009). Sedimentology, v. 56, p. 997-1015: Discussion, v. 58, p. 566-570

Higgs, R., 2014, New depositional model (lake-shelf hyperpycnites) for enigmatic Brushy, Cherry, and Bell Formations, Permian, Deleware Basin, USA: importance for local and global petroleum exploration and development. SW AAPG Convention,WTGS Publication, no.14-127, p. 26-38

Hollister, C., and Heezen, B., 1972, Geologic effects of ocean bottom currents: Western North Atlantic: Physical Oceanography, v. 15, p. 37-66

Hunter, R., and Clifton, H., 1982, Cyclic deposits and hummocky cross-stratification of probablestorm origin in Upper Cretaceous rocks of the Cape Sebastian area, southwest Oregon. Journal of Sedimentary Petrology, v. 52, p. 127-143

Jones, R., McCaffrey, K., Clegg, P., Wilson, R., Holliman, N., Holdsworth, R., Imber, J., and Waggott, S., 2009. Integration of regional outcrop digital data: 3D visualization of multi-scale geologic models. Computers and Geosciences, v.35, p. 4-18

Kreisa, R. D., 1981, Storm-generated sedimentary structures in subtidal marine facies with examples from the Middle and Upper Ordovician of southwestern Virginia. Journal of Sedimentary Research v 51.3

Lamb, M., Myrow, P., Lukens, C., Houck, K., and Strauss, J., 2008, Deposits from wave-influenced turbidity currents: Pennsylvanian Minturn Formation, Colorado, USA. Journal of Sedimentary Research, v. 78, no. 7, p. 480-498

Leckie, D., and Walker, R., 1982, Storm-and tide-dominated shorelines in Cretaceous Moosebar-Lower Gates interval--outcrop equivalents of Deep Basin gas trap in western Canada.AAPG Bulletin, v. 66, no. 2, p. 138-157

Lock, B., and Peschier, L., 2006, Boquillas (Eagle Ford) upper slope sediments, West Texas outcrop analogs for potential shale reservoirs: GCAGS, v. 56, p. 491-508

Lock, B., Peschier, L., and Whitcomb, N., 2010, The Eagle Ford (Boquillas) of Val Verde County, Texas- A window on the South Texas Play: GCAGS, v. 60, p. 419-434

Luca, P. H., and Basilici, G., 2013, A prodeltaic system controlled by hyperpicnal flows and storm waves: reinterpretation of the Punta Negra Formation: Brazilian journal of Geology, v. 43, no. 4, p. 673-694

Middleton, G. 1965, Antidune cross-bedding in a large flume. Journal of Sedimentary Research, v. 35, no. 4.

Midtgaard, H. M., 1996, Inner-shelf to lower-shoreface hummocky sandstone bodies with evidence for geostrophic influenced combined flow, Lower Cretaceous, West Greenland: Journal of Sedimentary Research, v. 66, no. 2, p.343-353

Molgat, M., and Arnott, R., 2001, Combined tide and wave influence on sedimentation patterns In the Upper Jurassic Swift Formation, south-eastern Alberta. Sedimentology, v.48, p. 1353-1369

Molina, J., Ruiz-Ortiz, P., and Vera, J., 1997, Calcareous tempestites in pelagic facies (Jurassic, Beltic Cordilleras, southern Spain. Sedimentary Geology, v. 109, p. 95- 109

Mulder, T., Razin, P., and Faugeres, J., 2009, Hummocky cross-stratification-like structures in deep- sea turbidites: Upper Cretaceous Basque basins (WesternPyrenes, France). Sedimentology, v.56, p. 997- 1015

Mulder, T., Razin, P., Faugeres, J., and Gerard, J., 2011, Reply to the Discussion by Roger Higgs on 'Hummocky cross-stratification-like structures in deep-sea turbidites: Upper Cretaceous Basque basins (Western Pyrenees, France)'by Mulder et al., Sedimentology, 56, 997–1015. Sedimentology, v. 58, no. 2, p. 571-577

Mrinjek, E., Pencinger, V., Sremac, J., and Lukšić, B., 2005, The Benkovac Stone Member of the Promina Formation: a Late Eocene succession of storm-dominated shelf deposits. Geologia Croatica, v. 58, no. 2, p. 163-184

Myrow, P. M., and Southard, J. B., 1991, Combined-flow for vertical stratification sequences in shallow marine storm-deposited beds: Journal of Sedimentary Petrology, v. 61, no. 2, p.202-210

Myrow, P., and Southard, J., 1996, Tempestite deposition. Journal of Sedimentary Research, v. 66, no. 5

Myrow, P., Fischer, W., and Goodge, J., 2002, Wave-modified turbidites: combined-flow shoreline and shelf deposits, Cambrian, Antarctica. Journal of Sedimentary research, v. 72, no. 5, p. 641-656

Nøttvedt, A., and Kreisa, R., 1987, Model for the combined-flow origin of hummocky cross-stratification. Geology, v. 15, no. 4, p. 357-361

Parker, G., 1982, Conditions for the ignition of catastrophically erosive turbidity currents. Marine Geology, v. 46, no. 3, p. 307-327.

Perillo, M., Best, J., Yokokawa, M., Sekiguchi, T., Takagawa, T., and Garcia, M., 2014, Aunified model for bedform development and equilibrium under unidirectional, oscillatory and combined-flows. Sedimentology, v. 61, no. 7, p. 2063-2085

Prave, A., and Duke, W., 1990, Small-scale hummocky cross-stratification in turbidites: a form of antidune stratification. Sedimentology, v. 37, p. 531-539

Quin, J., 2011, Is most hummocky cross-stratification formed by large-scale ripples?. Sedimentology, v. 58, no. 6, p. 1414-1433

Reineck, H., and Singh, I., 1975, Depositional Sedimentary Environments, Second Revised and Updated Edition, p. 35

Reineck and Singh, 1980, Depositional sedimentary environments. Springer-Verlag, New York, v. 549, p. 391-406

Ruppel, S., Loucks, R., Frebourg, G., (leaders), 2012, Guide to field exposures of the Eagle Ford- Equivalent Boquillas Formation and related Upper Cretaceous units in SouthwestTexas: Field seminar guidebook, p. 151

Rust, B., and Gibling, M., 1990, Three-dimensional antidunes as HCS mimics in a fluvial sandstone: the Pennsylvanian South Bar Formation near Sydney, Nova Scotia. Journal of Sedimentary Research, v. 60, no. 4

Sageman, B. B., 1996, Lowstand tempestites: Depositional model for Cretaceous skeletal limestones, Western Interior basin: Geology, v. 24, no. 10, p. 888-892

Seguret, M., Moussine-Pouchkine, A., Gabaglia, G., and Bouchette, F., 2001, Storm deposits and storm-generated coarse carbonate breccias on a pelagic outer shelf (South-East Basin, France). Sedimentology, v. 48, no. 2, p. 231-254

Snedden, J., Nummedal, D., and Amos, A., 1988, Storm- and fair- weather combined flow on the central Texas continental shelf. Journal of Sedimentary Petrology, v. 58, no. 4, p. 580-595

Simons, D., Richardson, E., and Albertson, M., 1961, Flume studies using medium sand (0.45 mm). Geological Survey Water-Supply Paper, no. 1498-A

Southard, J. B., Lambie, J. M., Federico, D. C., and Pile, H. T., Weidman, C. R., 1990, Experiments on bed configurations in fine sands under bidirectional purely oscillatory flow, and the origin of hummocky cross-stratification: Journal of Sedimentary Petrology, v. 60, no. 1, p. 1-17

Stow, D. A. V., 1979, Distinguishing between fine-grained turbidites and contourites of the Nova Scotia on deep water margin: Sedimentology, v. 26, p. 371-387

Swift, D., Figueiredo A., Freeland, G., and Oertel, G., 1983, Hummocky cross-stratification and megaripples: a geological double standard?. Journal of Sedimentary Research, v. 53, no. 4

Swift, D., Han, G., and Vincent, C., 1986, Fluid Processes and Sea-Floor Response on a Modern Storm-Dominated Shelf: Middle Atlantic Shelf of North America. Part I: The Storm-Current Regime, p. 99-119

Trevino, R. H., 1988, Facies and depositional environments of the Boquillas Formation, Upper Cretaceous of southwest Texas: M.S. Thesis, University of Texas at Arlington, p. 135

Trevino, R. H., and Smith, C. I., 2002, Facies and depositional environments of the Boquillas Formation: AAPG Annual Meeting, Article #90007

United States Energy Information Administration, 2013, Total Energy, Production, Eagle Ford 2013

Walker, R., Duke, W., & Leckie, D., 1983, Hummocky stratification: Significance of its variable bedding sequences: Discussion and reply Discussion. Geological Society of America Bulletin, v. 94, no. 10, p. 1245-1249

Wehner, M., Gardner, R., Xu, G., Pope, M., Staerker, S., and Donovan, A., 2013, The sedimentology, depositional environments, and correlation of the Eagle Ford Group (Boquillas Formation) in West Texas from Big Bend National Park to Maverick Basin: Unpublished transcript, Texas A&M Department of Geology and Geophysics, BP

Yamaguchi, N., and Sekiguchi, H., 2010, Effects of settling and preferential deposition of sediment on ripple roundness under shoaling waves. Journal of Sedimentary Research, v. 80, no. 9, p. 781-790

Yokokawa, M., Masuda, F., and Endo, N., 1995, Sand particle movement on migrating combined-flow ripples. Journal of Sedimentary Research, v. 65, no. 1